

University of Naples “Federico II”



PhD Programme: “Industrial Product and Process Engineering”

XXIX Cycle

**MULTILAYER HYDROGELS AS POTENTIAL STRATEGY
FOR *IN SITU* DRUG AND/OR CELL DELIVERY**

Author

Diogo Fernando Lopes Rodrigues

Tutor:

Prof. Antonio Gloria

Tutor/Coordinator:

Prof. Giuseppe Mensitieri

1 Table of Contents

1	State of the art	1
1.1	Introduction	1
1.1.1	Ischemia	1
1.1.2	Vascularization	3
1.1.3	Hypoxia and Angiogenic factors	5
1.1.4	VEGF	5
1.1.5	FGF	6
1.1.6	ECM	7
1.2	Therapeutic angiogenesis	7
1.3	Hydrogels	9
1.3.1	Hydrogels for Ischemia Applications	11
1.4	Self-assembling peptides	21
1.5	Synthetic Polymers	22
1.5.1	Poly(ethylene glycol)	22
1.5.2	Poly(N-isopropylacrylamide)	23
1.6	Micro- and Nano-particles	24
1.7	Dendrimers	28
2	Materials and Methods	30
2.1	Collagen gels	30
2.2	Collagen- LMWHA semi-Interpenetrating networks (s-IPNs)	30
2.3	Gelatin particles	31
2.4	Protein encapsulation within gelatin particles	31
2.5	Characterization of gelatin particles	32
2.6	Cumulative release of BSA from gelatin particles	32
2.7	Solid phase peptide synthesis (SPSS)	33
2.8	Functionalization of gelatin particles	34
2.9	Multilayer hydrogel	35
2.10	Rheological Analysis	36
2.11	Injectability tests	39
2.12	Cell adhesion study	40
3	Results and Discussion	44

3.1	Small amplitude oscillatory shear tests.....	44
3.2	Steady shear measurements.....	44
3.3	Injectability tests	45
3.4	Gelatin particles	47
3.5	Cumulative release of BSA from gelatin particles	49
3.6	Solid phase peptide synthesis (SPSS) and functionalization of gelatin particles.....	50
3.7	Multilayer hydrogels.....	52
3.8	Cell adhesion study	53
4	Conclusions	62
5	References	63

1 State of the art

1.1 Introduction

1.1.1 Ischemia

Cardiovascular diseases (CVDs) are the principal cause of death in the world (Figure 1), accounting for more than 17.3 million deaths per year. More than 15% of these deaths happened before the age 60 and could have been prevented. In Europe alone, over 4 million deaths occur each year due to CVD being the leading cause of death and loss of disability-adjusted life years (DALYS), a measure of overall disease burden. This disease affects both women and men being responsible for 42% of all deaths of European women and 38% of men below 75 years old [1]. Additionally, the treatment for CVD involves high costs in developed countries. For instance, in the United States in 2010, the medical costs were about \$273 billion and are expected to triple by 2030 [2].

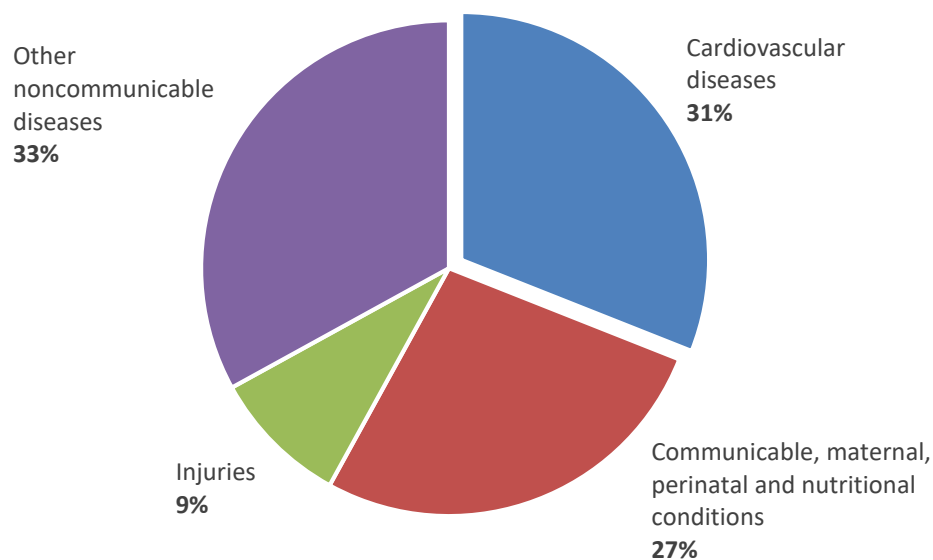


Figure 1 – Distribution of major causes of death, including CVDs.

CVD comprises diseases of the heart, vascular diseases of the brain and diseases of blood vessels. Among others disorders, CVD also includes ischemia which is characterized by

a suppression of blood supply to a tissue being the ischemic heart disease the main problem within CVDs and major cause of death of most western countries. Myocardial infarction (MI) may be connected to coronary heart disease (CHD) and it is defined as the myocardial cell death provoked by prolonged ischemia [3]. Ischemia can be caused by blockages due to an embolus or atherosclerosis resulting in tissue hypoxia and inflammation. When ischemia occurs, and thus an imbalance between oxygen supply and demand, a portion of the heart suffers ischemic necrosis and so a remodeling process starts in order to recover the cardiac loss. This process is responsible for modifications of myocyte biology, myocardial, extracellular matrix (ECM) and geometry of the left ventricular chamber. It has been divided into two phases: an early phase within 72 hours and a late phase, beyond 72 hours. As a result of following inflammation during the early phase, the infarct zone expands and human cardiac myocytes fails dealing to a defect on contractile function. In the late remodeling phase, as a result of collagen scar maturation, tissue fibrosis, distortion of ventricular shape and wall-thinning are experienced. Only when the tensile strength balances the distending forces of the heart the process is interrupted [4]. When blood supply is deficient to a limb, acute limb ischemia occurs which can deal to morbidity, amputation or even death when treatment is delayed [5]. Nowadays, therapies to treat ischemia include medications, percutaneous interventions and surgery. However, these strategies only diminish the symptoms and do not allow the tissue to regenerate and in more severe cases organ transplantation is the only alternative. Consequently, new strategies such as the use of minimally invasive injectable therapeutic hydrogels in order to promote neovascularization by delivering growth factors constitutes a promising approach to enhance blood flow, currently known as therapeutic angiogenesis [6]. Pro-angiogenic strategies may benefit more than 300 million people in the western countries [7].

1.1.2 Vascularization

The vessel growth is induced by several stimuli such as ischemia, hypertrophy, wound healing and inflammation [8].

Three processes contribute for the formation of new blood vessels: vasculogenesis, angiogenesis and arteriogenesis (Figure 2). The first one is connected to the formation of new blood vessels through the differentiation of endothelial progenitor cells (EPCs) or angioblasts in mature endothelial cells (ECs) creating primitive vessel networks. The EPCs can be derived from peripheral blood or bone marrow and are usually identified as CD34, Flk-1 or CD133 antigen-positive cells [9]. Angiogenesis is responsible for the formation of more complex vessels networks by the formation of new vascular structures from pre-existing ones. Accordingly, matrix metalloproteinases (MMPs) released by activated ECs degrade the surrounded extracellular matrix (ECM) forming new gaps to where cells migrate and sprout into novel blood vessels. ECs stimulation occurs by the action of vascular endothelial growth factor (VEGF) and basic fibroblast growth factor (bFGF). Hence, large caliber vessels can be subdivided into multiple new vessels, a process called intussusception process. Angiogenesis contributes to some physiological processes like wound healing, ovulation, placenta and ocular maturation [10-12]. Finally, arteriogenesis is responsible for the development and remodeling of pre-existing small arterioles into more caliber vessels. It occurs as a consequence of local changes in shear stress-induced accumulation of blood-derived mononuclear cells at the sites of arterial stenosis, occurring outside the ischemic area [8]. For a long time, it was believed that vasculogenesis process occurred only during embryonic development, now it's known that neovascularization in the adult includes both angiogenesis and arteriogenesis as well as a recapitulation of the embryonic processes. In adult life, endothelial cells, smooth muscle cells (SMCs) and other vascular cells are inactivated except when stimulated by inflammation, wounding, hypoxia or ischemia [6, 13, 14].

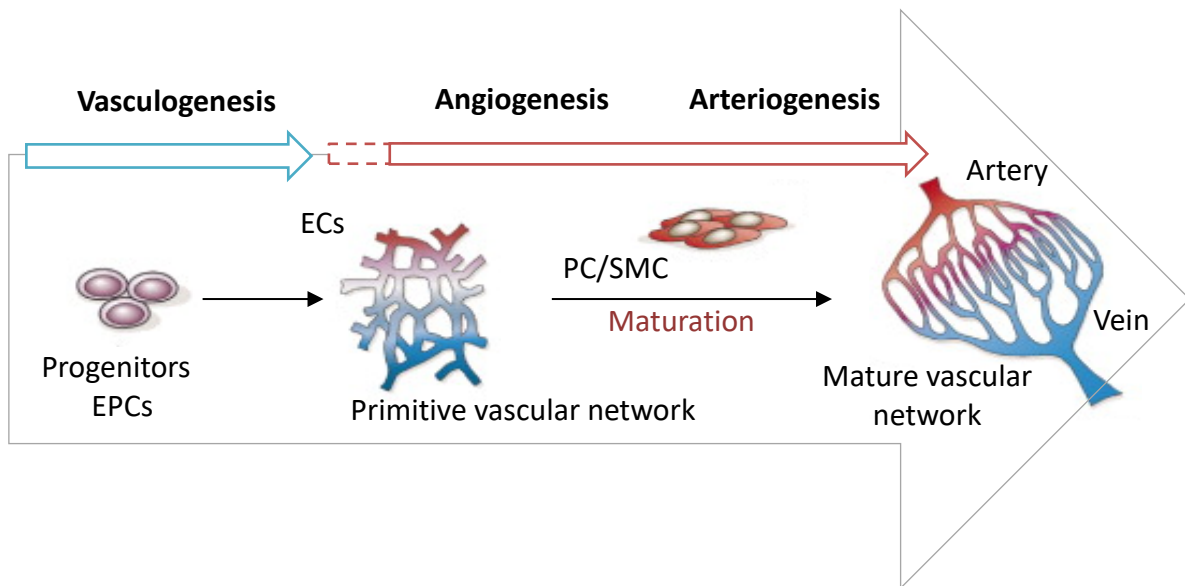


Figure 2 – Blood vessel formation. Adapted from [14].

Furthermore, maturation and stabilization of the new formed vessels are important in the formation of mature blood vessels and it is done by pericytes (PCs) and SMCs, suppressing also the endothelial cell growth. It happens through the action of growth factors such as platelet derived growth factor (PDGF) or angiotensin-1 (Ang-1). If this event doesn't occur as the blood vessels grow, they may suffer regression, be disorganized, permeable and hemorrhagic [15]. Consequently, when designing new vascularization approaches the moment on which maturation occurs is a relevant parameter. On one hand, if it occurs in an early stage, there will be no space for blood vessels elongation and not the whole tissue will be supplied with nutrients. On the other hand, if it begins too late vessels may probably regress and hence no functional blood vascularization will be formed [13].

1.1.3 Hypoxia and Angiogenic factors

Endogenous angiogenesis is stimulated by hypoxia or ischemia due to arterial occlusion. Subsequently, formation of additional vasculature is initiated by the combined work of upregulated angiogenic growth factors and activated cellular components on circulation [6, 16].

Vascular endothelial growth factor (VEGF), basic fibroblast growth factor (bFGF) and hepatocyte growth factor (HGF) have been identified as the most predominant factors in the upregulation of angiogenic processes, being the two firsts the most studied ones.

1.1.4 VEGF

VEGFs, a family of glycoproteins, promote angiogenesis by binding to its receptors on the surface of endothelial cells, stimulating the survival, growth and proliferation of vascular endothelial cells [17] as well as enhancement of its permeability and production of interstitial collagenase and plasminogen activators. In healthy humans, the levels of VEGF are low, increasing as a result of hypoxia and reactive oxygen species (ROS). It diffuses through the interstitial space binding to the ECM and surface receptors of cells and thus creating a gradient concentration which attracts endothelial sprouts towards hypoxic sites [7].

The VEGF family encompasses structurally related proteins: VEGF-A (VEGF-1 or simply VEGF), VEGF-B, VEGF-C (or VEGF-2), VEGF-D, VEGF-E and placental-derived growth factor (PlGF). Human VEGF-A monomers occur as 5 different isoforms: VEGF₁₄₅, VEGF₁₈₉, VEGF₂₀₆, VEGF₁₂₁ and VEGF₁₆₅ being this last one the most abundant and active form [18]. They differ by their heparin binding capacity. Longer VEGF isoforms (VEGF₁₆₅ and VEGF₁₈₉) bind heparin remaining more attached to the cell surface or to heparan sulfate of the ECM. Contrary, the shorter VEGF isoform (VEGF₁₂₁)

does not contain heparin-binding domains, is more soluble and doesn't bind to ECM [16]. Endothelial cells are the principal target of VEGF. VEGF can bind to three homologous membrane tyrosine kinases receptors: VEGFR-1 (Flt-1) and VEGFR-2 (KDR/Flk-1) expressed by blood vessels endothelial cells and VEGFR-3 (Flt-4) expressed by lymphatic endothelial cells [18].

The VEGF effect on angiogenesis is regulated at different stages. First, the expression of VEGF can be induced by various stimuli such as: HIF-1 α , growth factors and inflammatory cytokines. Then, co-receptors such as HSPGs and neuropilins as well as the interaction with adhesion molecules can control the duration and intensity of VEGFR signaling. Finally, HIF-1 α and TNF- α induces the transcription of VEGFR-2. The interaction between endothelial and SMC can also regulate VEGF signal [19].

1.1.5 FGF

FGF also induces EC proliferation and production of both collagenase and plasminogen activator [20]. Additionally, it induces proliferation of epithelial, mesenchymal and neural cell lines. In vitro, this growth factor interacts with specific co-receptor systems consisting of heparin-like glycosaminoglycans (HLGAG) and tyrosine kinase receptors (FGFRs) inducing cell proliferation, migration and production of proteases in ECs [6]. The binding of FGFs with HSPGs and glycosaminoglycans of the ECM produces a local pool of FGFs on cell surface and protects them from proteolytic degradation and denaturation. They use cell surface heparan sulphate proteoglycans to enable binding to tyrosine kinase receptors (RTK) inducing their dimerization and activation triggering signaling pathways important for cell growth and differentiation as well as for cell development, tissue maintenance and wound repair. At least 23 FGF ligands and seven FGFR have been identified in humans and mice. Acidic FGF (FGF-1) and basic FGF

(FGF-2) are the most studied and are involved in cardiac repair. Both receptors serve as ligands for SMCs and fibroblasts and are potent endothelial cell mitogens [6].

1.1.6 ECM

Besides the potential of growth factors, ECM plays also an important role on the formation and stabilization of new blood vessels. The interaction between ECM and cell is also important for cell maturation. Specific interactions between adhesion molecules on cell surface and ECM components allow a direct binding. ECM stimulates also morphogenesis and tissue repair by recruiting growth receptors that interact with cell surface receptors. In the case of angiogenesis, numerous ECM components, both soluble and insoluble, can bind angiogenic growth factors and release them as consequence of enzymatic ECM degradation mediated by cells. This process involves the development of gradients in vivo which can direct the formation of new blood vessels. Such gradients can be formed, for instance, by the connection of heparin sulfates and VEGF. So, knowing the role of ECM on both bind cells and release enclosed growth factors is essential when designing materials to guide tissue morphogenesis [9].

1.2 Therapeutic angiogenesis

Therapeutic angiogenesis constitutes a promising strategy to treat ischemic diseases and refers to the delivery of angiogenic growth factors to stimulate the growth and proliferation of new formed blood vessels. However, controlled release of the biomolecules must be achieved in order to let new blood vessels grow adequately and to avoid collateral effects [21]. For instance, when released in excess, VEGF has demonstrated to be responsible for vascular leakage that leads to edema and nitric oxide hypotension and unregulated formation of tumors [14]. Moreover, growth factors show

short diffusion distances through ECM because of their short half-life. VEGF has an *in vivo* half-life of around 50 minutes which may imply the injection of great amounts of VEGF to achieve the angiogenic effect and thus causing problems related to either the induction of vascularization in non-specific sites or tumor growth [22, 23]. So, new controlled release strategies may assure an accurate and constant release of growth factors over days or weeks and be active proximal to the desired angiogenesis site. In respect to VEGF, it has been shown its efficacy in promoting angiogenesis *in vivo* when administrated in engineered matrix polymers, microparticles or viral vector genetically encoding for VEGF [24]. Moreover, the matrix may mimic the complex role of the ECM in controlling the stability, activity, release and localization of growth factors.

Hydrogels have been used in order to overcome the main disadvantages of direct administration of growth factors, being possible to release it in a controlled manner and into the target sites. Strategies include physical entrapment of growth factors, covalent immobilization to the delivery system, non-covalent binding and the use of micro/nanospheres loaded with protein and embedded in hydrogels. Gene therapy, the delivering of genetic material encoded for the desired protein, and cell transplantation, encapsulation of cells which secrete specific proteins in a hydrogel, are two indirect approaches to release growth factors [22]. The success of VEGF delivering depends on the mechanism from which is incorporated into the hydrogel influencing its tissue distribution and exposure duration. Injectability plays a crucial role when it concerns hydrogels for drug releasing since it increases its effectiveness and limits further damage and invasiveness [25, 26].

1.3 Hydrogels

Hydrogels have demonstrated to be a promising polymer network for tissue engineering approaches because of their capacity to absorb great amounts of water, potential to be biocompatible and similarity to natural tissues [27, 28]. Injectable hydrogels represent an attractive drug delivery vehicle as they can be introduced *in situ* through minimally invasive ways and thus reduce the degree of damage upon delivery at the targeted area, require shorter procedures and recovery time [26]. After an MI event, a non-toxic *in situ* gelation process can be developed by injecting a liquid precursor into the myocardium [29]. However, the degradation properties and crosslinking density of the hydrogel must be manipulated to achieve sustained and localized release of growth factors. So, new approaches have been studied in order to control the release profile of the growth factors from hydrogels according to the cellular demands without changing its mechanic and physical properties [14, 30].

Hydrogels can be also used as three dimensional scaffolds to delivery cells. Vascular cells can be cultivated before transplantation allowing thus an enhancement of vascularization. Moreover, stem cell therapy offers therapeutic angiogenesis and treatment of ischemic diseases. However, when stem cells are placed in an ischemic tissue, cell survival is poor due to hypoxia conditions originated by deficiency of tissue vascularization leading to cell apoptosis and thus having a minor effect on the treatment of ischemia. Consequently, new approaches to improve cell survival and engraftment in ischemic sites have been studied. Among others, strategies include transplantation of stem cells in combination with growth factor delivery, genetic modification and use of tissue engineering scaffolds [31]. The success of cell therapy is determined by the capacity of the delivery system to localize and retain the cells in the damaged site while maintaining their survival for a long period. Three main aspects would make a biomaterial perfect for cell therapy:

introduction of an accurate cell population at the ischemic region; maintenance of their localization and survival over the period of treatment and production and release of specific factors into the ischemic site. So, one approach that has been studied is the formation of a cell-encapsulating hydrogel formed *in situ*. This strategy more than being non-invasive could allow the translation to clinical practice by using the existing catheter delivery technology [32].

Hydrogels are classified according to their polymer composition being divided into natural, synthetic polymer hydrogels and a combination of these two classes [33].

Natural hydrogels are constituted of proteins and take advantage over synthetic ones since they have components of the native extracellular matrix (ECM) and chemical structure like natural glycosaminoglycans, exhibiting excellent bioactivity and avoiding immunological responses. Moreover, naturally derived hydrogels present cellular binding domains allowing the regulation of cell behavior. However, most of these hydrogels show weak mechanical properties [34, 35].

Synthetic hydrogels, on the other hand, may have lower cellular bioactivity but show better chemical and physical properties allowing a higher control of ECM architecture and chemical composition [28]. In some cases, they are obtained from toxic chemicals and may show low degradation ratio at physiological conditions [36].

1.3.1 Hydrogels for Ischemia Applications

1.3.1.1 Natural Polymers

Natural hydrogels have been widely used as a drug delivery system of angiogenic cytokines since they favor biological events such as cell recruiting, regulation of inflammatory microenvironment and formation of neovasculature [37].

1.3.1.2 Alginate

Alginate is a natural occurring polysaccharide composed of (1-4)-linked β -D-mannuronic acid (M) and α -L-guluronic acid (G) monomers (Figure 3). When its chains get in contact with divalent cations, such as Ca^{2+} , gelation occurs due to the formation of ionic crosslinks. Gelation process results from the interaction of G-blocks with divalent cations [38].

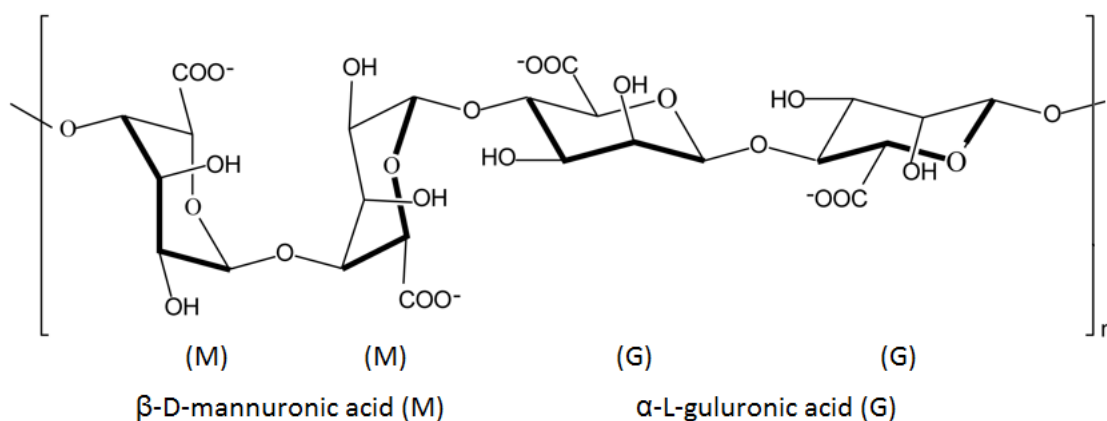


Figure 3 - Chemical structure of alginate, composed of (1-4)-linked β -D-mannuronic acid (M) and α -L-guluronic acid (G).

In the post-MI environment, a high concentration of calcium ions is present which can work as a local precursor to promote an *in situ* crosslinking mechanism. Then, as the post-infarction environment recovers the calcium concentration decreases, the alginate dissociates and may be clear from the region [32]. However, alginate deals with a fast initial release of hydrophilic drug molecules [39] and its degradation *in vivo* is slow and unpredictable due to the absence of enzymes that cleave the polymer chains. Still the manipulation of its mechanical properties and pores size is limited [22]. Modifications to

the polymer network can be done to obtain higher control on its degradation such as oxidation of polymer chains with sodium periodate. At partial levels of oxidation, gel biocompatibility is not altered. The control of molecular weight distribution of alginate constitutes another alternative to manipulate degradation of alginate gels by making it vulnerable to hydrolysis [38]. The combination of high and low molecular weight alginates followed by its partial oxidation and gamma irradiation was studied by Hao et al. They showed an increased angiogenic effect in a rat myocardial infarction model by releasing VEGF and platelet-derived growth factor-BB (PDGF-BB) in a sequential manner [40].

Moreover, its biocompatibility, low toxicity, similarity to ECM in tissues and ability to gel rapidly under mild conditions has motivated the use of alginate as an injectable system to deliver biomolecules or as a cell reservoir [28, 35]. Silva et al [41] produced an alginate injectable system and studied its potential to act as a reservoir system of bioactive VEGF. They showed the ability of this noninvasive and degradable system to control VEGF's biodistribution at appropriate concentrations for a long period (up to 15 days) in ischemic hind limbs and thus an enhancement of angiogenesis on the site of interest. The control of these two factors allowed an increasing on the tissue perfusion and thus prevention of necrosis associated with ischemia. Peters et al [42] demonstrated also a higher *in vitro* activity of alginate containing VEGF on ECs compared to the same amount added directly to the cells due to a higher stability of the growth factor when encapsulated within the alginate matrix.

Additionally, the functionalization of alginate with synthetic peptide sequences has been performed aiming an enhancement on cell anchoring and adhesion as cells don't have any specific receptors for binding to alginate and promote vascularization at ischemic sites. The arginine-glycine-aspartic acid (RGD) sequence is present in many ECM proteins

such as collagen, fibronectin, and laminin being responsible for cell attachment via integrins [43].

Yu et al. [44] immobilized alginate hydrogels with RGD peptides and studied its influence on the myocardial microenvironment and function in a rodent model of ischemic cardiomyopathy. Both in the presence or not of RGD modified group, alginate enhanced angiogenesis. However, a higher response was shown on the RGD modified alginate as it improved human umbilical vein endothelial cells (HUVEC) proliferation and adhesion indicating its influence at the infarcted myocardium microenvironment. Both hydrogels improved heart function after injection into the infarct area of rats 5 weeks post-MI.

1.3.1.3 Collagen

Collagen is the most abundant protein in the body and the principal constituent of ECM, being a potential biomaterial for tissue engineering applications. There are 28 different types of collagen being type I the most predominant [45].

Basically, all types of collagen present a triple helix structure which can form a microfibril by aggregation which, in its turn, can come together with others microfibrils to form a collagen fiber and collagen hydrogel [35].

Collagen gels physically formed are thermally reversible and show restricted mechanical properties. However, physical properties can be improved either by chemically cross-linking collagen using, for instance, glutaraldehyde, formaldehyde, carbodiimide and diphenylphosphoryl azide or by physical treatment crosslinking such as freeze-drying, UV irradiation and freeze-drying or by combination with other polymers (HA, PLA, PLGA, PGA, chitosan, PEO) [35, 46, 47].

This natural material contain specific amino acid consequences that can be recognized by cell receptors and are naturally degraded by metalloproteases such as collagenases and serine proteases [47]. Injectable collagen hydrogels can be produced by solubilizing the

collagen in an acidic manner. When injected *in vivo* at neutral pH and body temperature collagen crosslinks through fibrillogenesis forming a hydrogel capable of encapsulating cells. Even though it supports cell attachment, viability and proliferation, this process affects its structural properties, mainly elasticity and stiffness [32].

Collagen has been used also to deliver growth factors by hydrogels. Miyagi et al. [48] studied the promotion of vascularization by covalently immobilizing VEGF to a porous collagen hydrogel. The VEGF released from the collagen scaffolds led to an increasing of blood vessel density by enhancing cell proliferation within the hydrogel itself both *in vitro* and *in vivo*. Immobilized growth factors have shown to increase its stability and promote an effect localized in the hydrogel instead of in the surrounded tissue. Thus, this approach can allow a better transportation of both oxygen and nutrients into the growing tissue. Furthermore, the authors have shown suitable mechanical and biological properties of this system being a potential strategy for heart defects repair.

1.3.1.4 Gelatin

Gelatin is a biodegradable and denatured form of collagen which is obtained by hydrolysis, breaking the triple helix structure into single-strand molecules [28]. Gelatin shows both cationic and anionic ions with hydrophobic groups in the ratio of 1:1:1. Glycine, proline and hydroxyproline complete the rest of the chain. The triple helical structure is due to the representation $(\text{Gly-X-Pro})_n$, where X corresponds the amino acid, commonly lysine, methionine, arginine and valine. About 33% of the whole chain contains glycine, another 33% either proline or hydroxyproline and the remaining by other residues. Figure 4 depicts the primary gelatin structure, a polypeptide chain composed of 18 different aminoacids [49].

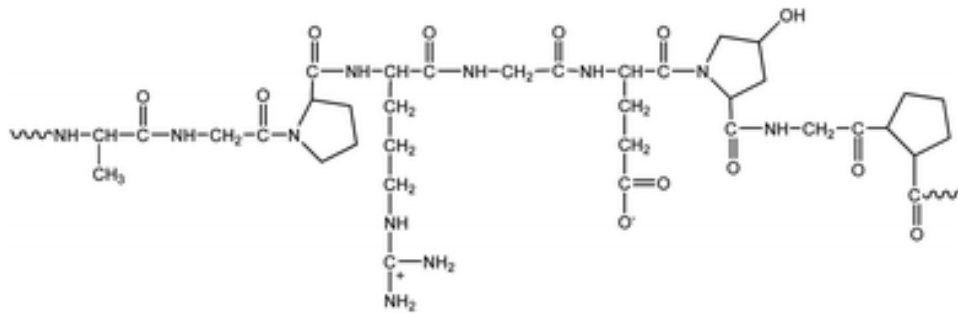


Figure 4 – Gelatin chemical structure in terms of aminoacids.

During the production process, the isoelectric point can be manipulated to obtain either a negatively charged acidic gelatin or positively charged basic gelatin at physiological pH [50]. Both gelatin types are available commercially. Cationic gelatin (gelatin type A) is prepared by an acidic hydrolysis of pig skin type I collagen, showing an isoelectric point of 7-9. Contrary, anionic gelatin, commercially known as gelatin type B, shows an isoelectric point of 4.8-5 and is obtained by an alkaline hydrolysis of bovine collagen [49].

Gelatin hydrogels have been used as delivery systems of angiogenic molecules since Thompson et al. used it for the first time to deliver acidic FGF [51]. The release of acid FGF occurs as a result of the *in vivo* degradation of the hydrogel [52, 53] and the releasing profile can be manipulated by varying the water content of the hydrogel [53]. Both electrostatic interactions between the gelatin and the growth factors and the type of gelatin (basic or acid) influence either there is a controllable release of the biomolecules or not [54]. Several reports have demonstrated the bFGF-incorporating acidic gelatin hydrogel potential to improve angiogenic effects, in contrast to bFGF in solution [55, 56]. Moreover, in order to study the safety and application of gelatin hydrogels releasing bFGF on patients with critical limb ischemia, a clinical trial has been started recently [57]. Strategies including covalent attachment of heparin to collagen, manipulation of the amount of glutaraldehyde used and thus degradation rate have been taken in consideration

to control the initial high burst release of growth factors and increase the growth factors loading capacity into gelatin [54, 58].

1.3.1.5 Hyaluronic Acid

Hyaluronic acid (HA) is a naturally occurring non-sulfated glycosaminoglycan consisting of repeating disaccharide units of β -(1-4)-linked guluronic acid and β -(1-3)-linked *N*-acetyl-*D*-glucosamine (Figure 5) with a molecular weight ranging from 100 to 5000kDa and is present in the ECM of mammalian tissues.

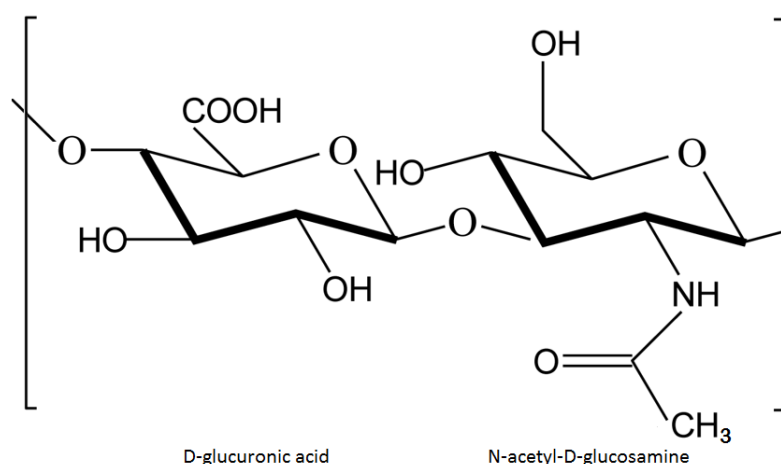


Figure 5 – Chemical structure of hyaluronic acid, composed of β -(1-4)-linked guluronic acid and β -(1-3)-linked *N*-acetyl-*D*-glucosamine.

Low molecular weight HA stimulates endothelial cell proliferation and spreading while the high ones have inhibitory angiogenic effects [59]. It's degraded by hyaluronidase and despite of being biocompatible, biodegradable and with excellent gel-forming properties, shows poor mechanical properties in its native form. Therefore, modifications are performed to obtain HA cross-linked networks and, consequently, achieve better properties in terms of hydrophobicity and biological activity. The most widely used are the chemical modifications such as esterification, crosslinking with hydrazide derivates and annealing. While increasing the mechanical and processability properties, these

chemical modifications may compromise its biological activity. Xin et al [60] have produced a collagen-HA semi-interpenetrating gel by allowing the collagen fibrillogenesis occur in the presence of HA molecules with different molecular weights. Results demonstrated the influence of the molecular weight on the mechanical properties which increased in the presence of low molecular weight hyaluronic acid (LMWHA), corresponding to a molecular weight of 155×10^3 .

HA plays important roles in cellular signaling, morphogenesis, wound repair, matrix organization and it is able to promote angiogenesis and suppress fibrous tissue formation showing its potential as cardiac biomaterial [28, 35, 61]. Abdalla et al. [62] have shown the potential of acellular hyaluronic acid-based hydrogel to increase cardiac function post-myocardial infarction in a rat model. An improvement in cardiac function was observed up to 3 weeks in the injection fraction, there was an increase in new vasculature formation and a decrease scarring and collagen deposition.

1.3.1.6 Fibrin

Fibrin is a fibrous protein and the major component of blood clots. Its precursor is fibrinogen which, under certain conditions, polymerizes into fibrin. Upon tissue bleeding, fibrinogen is converted into fibrin by the action of the proteolytic enzyme thrombin. Thrombin converts fibrinogen into fibrin in 10-60 seconds [11]. Fibrin-based materials are biocompatible and have been used as tissue scaffold, cell and angiogenesis support. However, natural fibrin gels present low mechanical strength so it must be seeded for long periods of time to enhance their properties. Alternatively, by increasing fibrinogen concentration, gelation times are faster resulting in a tighter network which may lead to an improvement of mechanical properties. Cell-seeded fibrin scaffolds with elastic moduli of around 10-30kPa, a range suitable for myocardial tissue applications, have been obtained by varying the concentration of thrombin [32]. Nevertheless, over a threshold

concentration it can be prejudicial for cell surviving and spreading. It has been reported that this protein-based hydrogel has the ability to promote angiogenesis by itself through the release of degradation products which are non-immunogenic amino acids products [63-65]. Christman et al [64] showed the potential of fibrin glue to treat ischemic myocardium since its injection after one week of MI induction in a rat model of ischemia showed an increased cell transplant survival and retention, induction of neovasculature formation, decreasing infarct size and increased blood flow to ischemic myocardium and thus improvement in cardiac function.

Growth factors can be loaded into fibrin network, for instance, by physically mixing them with fibrinogen and thrombin during coagulation. However, a drawback relies on an initial rapid release (within 24h) and consequently a rapid clearance of the growth factors. So, new strategies have been studied to control the release kinetics of growth factors. One approach consists on the incorporation of growth factors to fibrin by transglutaminase activity of factor XIIIa during coagulation [9]. Another one consists on the immobilization of heparin within the fibrin network since most of angiogenic factors are heparin-binding peptides. Chung et al [23] developed a VEGF-loaded nanoparticle-fibrin gel complex showing an increased angiogenic bioactivity in respect to collateral density in a rabbit ischemic hind limb model.

1.3.1.7 Matrigel

Matrigel is constituted by a complex protein mixture comprising laminin, collagen IV and heparan sulfate proteoglycans [28]. It is produced by mouse tumour cells and constitutes one of the most used materials to evaluate the potential of cells and growth factors to promote angiogenesis [66]. It presents a combination of various angiogenic growth factors such as VEGF, insulin-like growth factor I (IGF-1) and epidermal growth factor (EGF) which favor the development of new blood vessels and also platelet-derived

growth factor (PDGF) and transforming growth factor (TGF)- β which are responsible for the maturation of newly formed blood vessels [67].

Schumann et al. [68] used Matrigel-filled PLGA scaffolds preincubated either with osteoblast-like cells (OLCs) or mesenchymal stem cells (bmMSCs) and the combination of both to study their effects on the vascularization process in tissue engineering scaffolds *in vivo*. The host tissue response in respect to angiogenesis and inflammatory processes was studied. Both scaffolds seeded with bmMSCs and both cell types showed an improved development of microvascular networks being more predominant between day 3 and 6 after implantation.

One disadvantage of this material, however, is the batch to batch variability and possible tumor formation after implantation since it is derived from a mouse sarcoma line [69].

1.3.1.8 Chitosan

Chitosan is polysaccharide obtained by deacetylation of chitin, a naturally occurring source present in crustaceans, insect's exoskeleton and fungi. The conditions used in the process of deacetylation will define the polymer molecular weight and the degree of deacetylation [70]. Chitosan is a linear copolymer which contains β -(1,4)-linked D-glucosamine and *N*-acetyl-D-glucosamine molecules (Figure 6) which facilitates electrostatic interactions with naturally occurring glycosaminoglycans (GAGs) and proteoglycans of the ECM [28].

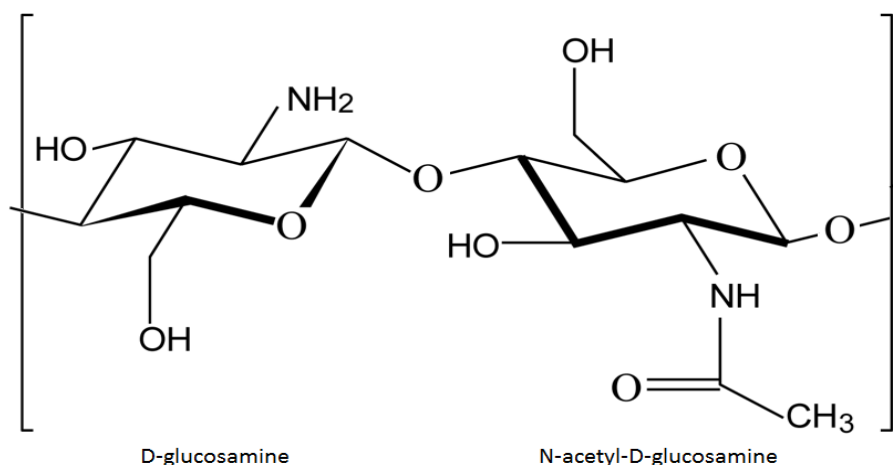


Figure 6 – Chitosan chemical structure, composed of β -(1,4)-linked D-glucosamine and N-acetyl-D-glucosamine.

Since this polysaccharide can be obtained from abundant natural and renewable resources and be chemically and physically modified, it has been investigated for many tissue engineering applications. It's biocompatible, biodegradable, has low immunogenicity and it's positively charged due to the presence of amine groups. Thus, chitosan is soluble in acidic solutions and can form a hydrogel via UV radiation, glutaraldehyde crosslinking or thermal variations [35, 70]. Chitosan hydrogels respond to different external stimuli such as temperature, pH and light. For instance, an injectable hydrogel combining the temperature-responsive chitosan and glycerol phosphate (GP) may be very attractive as a drug delivery system. This combined polymer solution allows the incorporation of bioactive factors which can be trapped within the injected area when exposed to body temperature due to rapid polymerization [28]. Moreover, the degradation of chitosan *in vivo* by lysozyme produces oligosaccharides which have been shown to enhance vascular endothelial cell migration and angiogenesis [32]. Biomaterials aimed to be applied in ischemic sites must be injectable and capable to overcome or minimize the hostile environment generated by the ischemic region such as lack of angiogenesis, inflammation, reactive oxygen species (ROS) [71, 72]. Liu et al [71] developed an injectable thermoresponsive chitosan hydrogel for stem cell delivery into ischemic heart

evidencing the efficiency of this system to alter the myocardial infarction microenvironment and hence enhance cell engraftment, survival and homing.

1.4 Self-assembling peptides

Self-assembling peptides (SAPs) are oligopeptides composed of alternating hydrophilic and hydrophobic amino acids and thus highly soluble in water. Normally, SAPs form stable β -sheet structures in water. When exposed to physiological salt concentrations they can form hydrogels. These materials are appropriate for tissue engineering applications as they can support cell attachment and differentiation of a diversity of tissue culture and mammalian cells under physiological conditions due to the formation of an extracellular matrix like structure [73, 74]. Moreover, their chemical composition and mechanical strength can be manipulated by controlling peptides parameters [75, 76]. Accordingly, higher G'/G'' ratio may stimulate longer cell-cell interactions resulting in more extended and larger structures when compared to those obtained with lower G'/G'' ratio which were smaller and denser. Similarly, modification of the mechanical properties allows the improvement of pore size and capillary formation [77]. SAPs can be applied for protein delivery as they are able of binding clinically relevant levels of growth factors [32]. Thus, studies have been demonstrating the ability of these self-assembly scaffolds to promote angiogenesis by providing cells with a soft three-dimensional support. For instance, Kim et al [78] demonstrated an increasing of angiogenesis for treatment of myocardial infarction by controlling the dual release of growth factors (FGF-2 and PDGF-BB) and its stability from SAPs into ischemic areas.

1.5 Synthetic Polymers

Synthetic hydrogels show various advantages in comparison to the natural ones. Their mechanical and degradation properties can be easily and precisely tunable; they show batch-to-batch consistency and offer availability to be chemically functionalized. Conversely, they lack the innate bioactivity characteristic of natural polymers, compromising cellular interactions such as adhesion, proliferation and remodeling [32].

1.5.1 Poly(ethylene glycol)

Poly(ethylene glycol) (PEG) is being used as a synthetic matrix in tissue engineering since it's highly hydrophilic, presents low immunogenicity and protein adsorption and has demonstrated safety on *in vivo* uses [79]. PEG-based hydrogels can be obtained by covalently crosslink PEG polymers through different methods. The most common method consists on photopolymerization of acrylate functionalized PEG monomers. However, this process makes use of UV which can be harmful for cells and results in materials with no controllable structures. Thus, hydrogels formed through Michael-type addition reaction constitute an alternative since it's performed under physiological conditions. For vascularization applications, modifications to PEG must be done such as chemical bioconjugation. Peptide sequences have been coupled to the polymer in order to improve its cell adhesion or degradability. For instance, RGD sequences have been used to allow cell adhesion [80].

Kraehenbuehl and colleagues [81] produced a PEG hydrogel via Michael-type addition reaction of thiol-containing peptides onto vinylsulfone-functionalized PEG. MMPs were added to the peptides sequence in order to allow the hydrogel degradation and remodeling along with RGDSP cell adhesive ligand. Thus, the potential of this MMP-responsive PEG-based hydrogel to encapsulated both thymosin β 4 (T β 4), a pro-angiogenic and pro-

survival factor, and HUVEC was studied. Gels with entrapped T β 4 showed an increased number of attached HUVECs and acceleration of vascular-like network formation. It also allowed the up-regulation of cadherin and angiopoietin-2 and secretion of MMP-2 and MMP-9 from encapsulated HUVECs and thus controlled release of T β 4 from the system. This system can be useful for *in situ* regeneration of ischemic tissues where the expression and activation of MMPs is increased. More than chemical modifications, similar polymers can be added to obtain specific properties.

1.5.2 Poly(N-isopropylacrylamide)

PNIPAAm is a temperature sensitive hydrogel which undergoes a reversible phase transition from sol to gel at physiological temperature conditions due to its lower critical solution temperature (LCST) of around 32°C. Therefore, it enables a rapid gelation *in situ* when injected being a potential strategy for cardiac tissue engineering. This thermoresponsive polymer allowed the release of VEGF to human vascular endothelial cells for a long period of time [82].

As for PEG, this material shows low bioactivity and it is non degradable since its LCST remains constant being not cleared by the body. Thus, this polymer is often modified by combining it with other polymers such as collagen, hyaluronic acid and gelatin [83-85] or biomolecules [86].

When tested *in vitro* most systems provide a sustainable and controllable release of angiogenic factors as well as a functional improvement at early time points. Therefore, it constitutes a drawback for clinical implementation where there is the influence of the surrounding environment such as changes in pH due to ischemia and fluctuations in extracellular milieu as a result of the inflammatory response [21]. Consequently, the incorporation of carboxylic acid-derived monomers has been useful to modify the LCST

and respond to acid conditions. Garbern et al. [21] developed an injectable, pH and thermoresponsive hydrogel based on the copolymerization of N-isopropylacrylamide (NIPAAm), propylacrylic acid (PAA) and butylacrylic (BA) (p[NIPAAm-co-PAA-co-BA]) for therapeutic angiogenesis. At pH 6.8 and 37°C this polymer forms a gel being suitable for drug delivery in ischemic sites which are regions with an acidic environment (pH 6-7) and eliminated once the ischemic conditions are reduced. p[NIPAAm-co-PAA-co-BA] was used to deliver bFGF *in vivo* immediately post-MI in a rat and compared to saline, polymer alone and bFGF in saline. Contrary to bFGF in saline and polymer itself where no effects were observed, this system showed a 2-fold improvement in blood flow after 28 days. In addition, there was an increasing in 30-40% on capillary and arteriolar densities. The cardiac function was also enhanced since both angiogenesis and thickness of the infarcted wall were improved. However, the increased wall thickness was increased by using the polymer alone which may be connected to collagen deposition due to inflammatory responses.

1.6 Micro- and Nano-particles

Hydrogels show biocompatibility and high inertness to protein drugs which make them a great candidate as a protein release network. However, they can suffer chemical modifications and thus reduce the bioactivity of functional moieties; experience irreversible complexation and retain residual cross linkers dealing with the denaturation of growth factors and induce of immune responses or acute inflammation [23]. Consequently, controllable release of proteins from hydrogels may not be accomplished since it's a process mainly diffusion-controlled. Hence, the use of loaded micro (>1µm and <1000µm sized) or nanoparticles (<1µm sized) [87] embedded in hydrogels has been

used as a strategy to multimodal protein delivery. These systems are developed to release drugs over time in a sustained and controllable manner, to diminish the number of doses needed to treat the disease and to allow biomolecules to reach the target site without being inactivated [88]. Microparticles are capable of providing sustained release kinetics after implantation and their diffusion from the implantation site is unusual avoiding collateral effects in adjacent tissues. Nanoparticles, instead, can internalize the cells through capillaries [87]. Polymeric microparticles take advantage, for instance, over osmotic pumps as no surgical procedures are needed for their application or removal from the body; they are more stable than liposomes at biological conditions and they allow the encapsulation of hydrophilic and hydrophobic molecules [88].

For instance, poly (d,l-lactide-co-glycolide) (PLGA) microparticles have been widely used as growth factor delivery systems for angiogenesis and have shown to improve blood vessel formation in tests performed in hindlimb ischemia models [89, 90].

Lee et al. [39] developed a microsphere/hydrogel combination system to increase angiogenesis *in vivo* by promoting the release of bioactive molecules. This system was composed by PLGA microspheres and alginate hydrogels loaded with rhVEGF. The ratio influence of PLGA microspheres and hydrogel on the release profile of rhVEGF was studied being more controllable as the amount of microspheres increased. No cytotoxicity was showed against endothelial cells showing the possibility to be used *in vivo* as an injectable delivery system. When used at small doses *in vivo* this combination showed to improve the formation of new blood vessels.

Des Rieux et al. [25] studied whether the encapsulation of VEGF into dextran sulfate/chitosan nanoparticles could increase angiogenesis *in vivo* when compared to its free incorporation into matrigel hydrogels and PLGA scaffolds. Regardless the VEGF dose, implantation type and time, results have shown a better colonization of endothelial

cells and blood vessel formation when VEGF was incorporated within the nanoparticles in comparison to those obtained when it was added freely into the matrices.

Gelatin microparticles have been used also as a carrier for controlled release such as bFGF, transforming growth factor (TGF- β 1), insulin-like growth factor-1 and bone morphogenetic protein-2 (BMP-2). Growth factors are released through an enzymatic degradation of the gelatin by the action of matrix metalloproteinases such as collagenase. The crosslink degree can influence the degradation rate and consequently the release profile. Patel et al [54] studied the efficacy of acidic gelatin microparticles to release VEGF in a controllable manner by varying the gelatin crosslinking degree, the amount of VEGF and release medium *in vitro* and *in vivo*. Results have demonstrated the potential of gelatin microparticles to deliver VEGF over 4 weeks in a dose independent manner. The addition of collagenase increased the VEGF release confirming its degradation through an enzymatic-driven process. A controllable release profile was achieved, both *in vitro* and *in vivo*, by manipulating the crosslinking extent.

Gelatin nanoparticles represent also a favorable vehicle system for controllable drug release. They can be obtained, for instance, by techniques including: desolvation, coacervation-phase separation, emulsification-solvent evaporation, reverse phase microemulsion, nanoprecipitation, self-assembly and layer-by-layer (LbL) coating. The coacervation method is a process of liquid-liquid separation followed by a crosslinking step. This method shows a poor loading efficiency and non-homogeneous crosslinking. The emulsion-solvent evaporation technique is based on water-in-oil emulsion process. Large quantities of surfactant are necessary to obtain small-sized particles, requiring a complex post-process. In fact, these methods showed to be responsible for the production of large and heterogeneous particles because of the discrepancy of molecular weight of the gelatin polymer. So, desolvation was found to be an adequate method to produce

gelatin nanoparticles. This method begins with the dehydration of gelatin molecules by the addition of a desolvating agent such as alcohol or acetone. However, this first step of desolvation produces large particles with a high polydispersity index (PDI) because of the heterogeneity in molecular weight of gelatin. By performing a second step of desolvation, smaller and more homogeneous gelatin particles are formed [91]. This occurs because after the first step of desolvation, there is deposition of the high molecular weight (HMW) gelatin and so the low molecular weight (LMW) gelatin can be removed. Then, the precipitated HMW is redissolved and desolved again (second step of desolvation). Finally, to harden the nanoparticles, a step of crosslinking is essential. This last step represents one of the disadvantages of this method as well as the use of organic solvents [49].

Glutaraldehyde (GA) is normally used as a crosslinker for gelatin nanoparticles. It is a non-zero length crosslinker which binds to free amino groups of lysine and hydroxylysine residues. One disadvantage of using this crosslinker is the possibility to initiate undesired immune or toxicological responses [49]. Gelatin nanoparticles produced through this method showed an average particle size between 250-300 nm with a homogeneous size distribution (PDI 0.02) [92].

Gelatin nanoparticles have been encapsulated with bovine serum albumin (BSA), they can absorb large amounts of water (51-72%) and the release of BSA from these nanoparticles follows a diffusion controlled mechanism [93]. The release mechanism of hydrophilic proteins may involve water infusion and adsorption by the nanoparticles, swelling and finally diffusion of BSA molecules [94]. Encapsulation of drugs into nanoparticles can be accomplished either by adding the drug at the time of nanoparticle production or by drug adsorption after nanoparticle formation through its incubation in the drug solution [93]. Won et al [95] have demonstrated a sustained and reduced burst

release of FITC-BSA from recombinant human gelatin (rHG) nanoparticles. Li et al [96] have produced a system composed of gelatin nanoparticles loaded with BSA encapsulated into PLGA microspheres which was able to release the molecule in a controllable manner and to avoid its denaturation.

bFGF was also encapsulated into gelatin nanoparticles showing a controlled release more dependent on the crosslinking degree than on the type of gelatin [97].

1.7 Dendrimers

The growth factors delivery systems described before constitute the most studied and versatile ones but there are others which have been also used to delivery growth factors such as dendrimers.

These are a class of synthetic, well-defined hyperbranched polymers of nanometer dimensions that resemble, at molecular level, the architecture of a tree. Three distinct structural regions can be described in a typical dendrimer structure: a multifunction central core; branched monomeric units organized in layers called “generations” (G_n) and external functional groups which are important in their properties and designed to offer functionality to the dendrimer. Dendrimers are produced in a layer-by-layer fashion (generations - G_n), being the size dependent on monomer layers. By the removal of the functional core, identical fragments called dendrons remain (Figure 7). Dendrons of higher generations present more branches and terminal groups being larger macromolecules in respect to those of lower generations [98, 99].

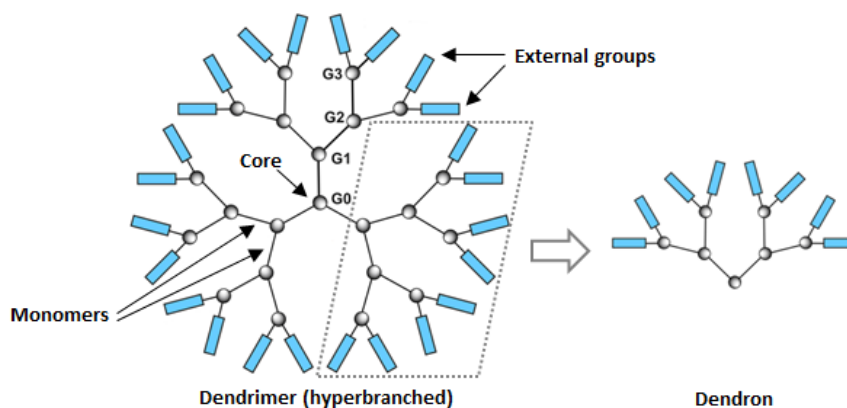


Figure 7 – Basic structure of a dendrimer and dendron.

Dendrimers can be prepared by two different synthetic approaches which main difference relies on the direction of dendrimer growth: the divergent and convergent method. In the divergent method, the dendrimer grows in a stepwise manner by the addition of successive branching units from a core molecule. In the convergent method, instead, the opposite sequence is performed: the dendrimer growth starts from the end groups towards the inside being finalized by the addition of a central core [100]. The ability to control properties such as size, branching points and surface functionality make dendrimers an ideal candidate as vehicles to deliver biomolecules and small drugs. Dendrimers are biocompatible, high soluble, can encapsulate drugs and present nano-scaffolding properties as surface adsorption or attachment of a drug [99].

2 Materials and Methods

2.1 Collagen gels

Collagen solution from bovine skin (Sigma Aldrich) and rat tail collagen high concentration (HC), TYPE 1 (BD Bioscience) were used in this study.

Collagen gels were prepared by diluting the collagen solution in Dulbecco's Modified Eagle's Medium (DMEM). In detail, collagen was mixed with DMEM, subsequently 0.1 M NaOH solution was added and mixed to obtain a specific collagen concentration. The pH of the solution was then adjusted to 7.4 ± 0.2 . The solution was properly diluted providing a final collagen concentration of 1.2 mg/ml or 4 mg/ml. The solution was then incubated in a thermostatic bath at 37°C for 1 h to allow collagen fibrillogenesis. During the incubation, the atelocollagen molecules assemble to each other to form collagen fibres, and after 1 h a firm collagen gel was obtained.

2.2 Collagen- LMWHA semi-Interpenetrating networks (s-IPNs)

Collagen-LMWHA s-IPNs were obtained by promoting collagen fibrillogenesis in the presence of LMWHA. LMWHA powder dissolved in DMEM was suitably mixed with the collagen solution, thus obtaining a final LMWHA concentration of 2.5 mg/ml (and a collagen concentration of 1.2 mg/ml or 4 mg/ml). The solution was incubated at 37°C to allow collagen fibrillogenesis. After the incubation, the collagen was completely fibrillated and collagen-LMWHA s-IPNs were obtained.

2.3 Gelatin particles

Gelatin particles (GPs) were prepared using a two-step desolvation method reported by Coester et al. Briefly, 1.25 g of gelatin type A from porcine skin was dissolved in 25 ml of distilled water under heating (37°C) along with magnetic stirring (300 rpm). 25 ml acetone was added to the gelatin solution as a desolvation agent. Then, the supernatant was discarded and the remaining sediment was redissolved by adding 25 ml of water with stirring under constant heating and the pH adjusted to 3.0. Gelatin was again desolvated by drop-wise addition of 75 ml of acetone to form the particles. At the end of the process, 500 µl of glutaraldehyde (8%) was added as crosslinking agent and the solution was stirred overnight. The particles were purified by threefold centrifugation and redispersion in acetone/water (30/70). After the last redispersion, fabricated particles, were freeze-dried and stored at room temperature.

2.4 Protein encapsulation within gelatin particles

Gelatin particles were produced by the classical two-step desolvation method as described before. To achieve Bovine serum albumin (BSA) loading by matrix incorporation, BSA was added to the formulation during the second desolvation step. Different concentrations of BSA were added (0.2%, 0.5%, 1%, 2% and 5% w/w) and dissolved in the pH adjusted gelatin solution, followed by dropwise addition of acetone to form gelatin particles. 500 µl of glutaraldehyde (8%) was added and the solution left to crosslink overnight. The particles were purified by threefold centrifugation and redispersion in acetone/water (30/70). After the last redispersion the particles were freeze-dried and stored at 4°C.

In the same manner, as a final stage of the research activity, VEGF- and PlGF-loaded gelatin particles were also obtained.

2.5 Characterization of gelatin particles

Gelatin particles were characterized in terms of mean particle size and morphology using a Zetasizer Nano ZS (Malvern Instruments) and scanning electron microscopy (FEI Quanta 200 FEG).

2.6 Cumulative release of BSA from gelatin particles

The releasing profiles of BSA from gelatin NPs were monitored by the UV-Vis spectrophotometer (Perkin Elmer) at 278 nm. Briefly, gelatin particles were suspended in Phosphate Buffer Solution (PBS, 10 mg/ml) and allocated in an orbital shaker at 37°C. The release sample was collected at regular time intervals, after centrifugation (8000 rpm for 15 min) and re-dispersion in fresh phosphate buffer solution (PBS). All the points for each time interval were measured in triplicate. A standard curve was plotted to represent the correlation of the concentration of BSA and the corresponding intensity of the absorbance in the UV-Vis spectra.

The BSA release was evaluated as follows:

$$BSA \text{ release } (\%) = 100 \frac{M_t}{\sum_{t=0}^{t=\infty} M_t}$$

where M_t represents the amount of BSA released at the time t .

2.7 Solid phase peptide synthesis (SPSS)

Solid phase peptide synthesis is the most common method used for peptide synthesis. In this work, the tethered poly (ϵ -lysine) dendrons of three (G3K) branching generation type were synthesised on a Tenta Gel S (-NH₂) resin using a 9-fluorenylmethoxycarbonyl (Fmoc) solid phase peptide method. Di-phenylalanine (FF) were used as core molecules. 0.50 g of resin was placed inside a syringe and swollen in N, N-dimethylformamide (DMF) for 10 min. Resin was attached to the C-group of a fourfold excess of a rink amide linker mixed with 0.152 g of O-Benzotriazole-N,N,N',N'-tetramethyl-uronium-hexafluoro-phosphate (HBTU), 3 ml DMF and 140 μ l of 33% v/v N,N-diisopropylethylamine (DIPEA) for 40 min which are used as activators. Then, a deprotection step was done to remove the base-labile Fmoc-group by washing 3 times with 2 ml of 20% v/v piperidine and twice with DMF. The exposure of a new N-terminal amine allowed the assembly of a series of Fmoc-amino acids (Table I).

Addition Step	Amino acid	No. cycles (0.4mmol)	Reactive sites at start/end of cycle (nmol)	Molar Excess
Rink Amide	Fmoc Rink Amide Linker	1	0.1/0.1	4
FF	Fmoc-Phe-OH		0.1/0.1	
G0	Fmoc-Lys(Fmoc)-OH		0.1/0.2	
G1	Fmoc-Lys(Fmoc)-OH	2	0.2/0.4	
G2	Fmoc-Lys(Fmoc)-OH	4	0.4/0.8	
G3	Fmoc-Lys(Fmoc)-OH	8	0.8/1.6	

Table I - Assembly sequence of FFG3K.

After the addition of all amino acids by a series of coupling and deprotection steps, the peptide was allowed to stand for 30 minutes for a final deprotection in 4 ml of 20% piperidine. Then a series of washes were done: 4 times with 8 ml of dichloromethane; 4 times with 8 ml of methanol and 4 times with 8 ml of diethyl ether. The product of synthesis was then dried overnight under the hood and weighed. The final cleavage of the synthesised peptide from the Tenta Gel resin was obtained by the introduction of a linker bearing an ester moiety which is susceptible to cleavage by trifluoroacetic acid (TFA). The synthesis of the dendrons was confirmed by mass spectrometry.

2.8 Functionalization of gelatin particles

The attachment of the FFG3K peptide to the gelatin particles was performed by using 1-ethyl-3-(3-dimethyl aminopropyl) carbodiimide (EDC) and *N*-hydroxysuccinimide (NHS) (Figure 8). Briefly, FFG3K peptide was activated by mixing with 0.1 M MES (2-[morpholino]ethanesulfonic acid) at pH 6.0, EDC and NHS. The mixture was shaken gently for one hour at 37°C. Thus, FFG3K peptide was added and kept under shaking overnight at 37°C. After the incubation period, the particles were purified by threefold centrifugation at 6000 rpm for 20 min and washed with water.

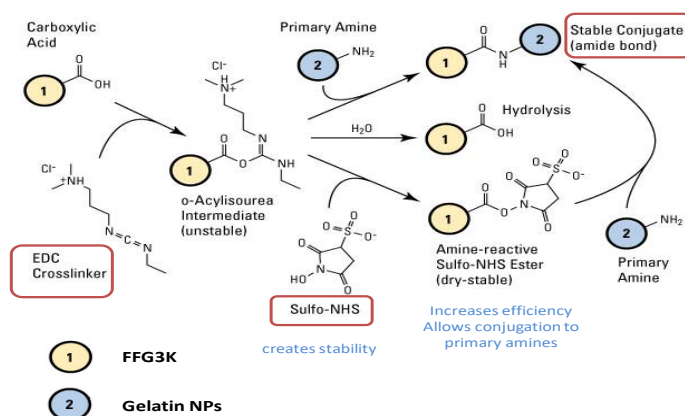


Figure 8 - A schematic representation of the functionalization process.

Functionalized gelatin particles were characterized by attenuated reflectance Fourier transform spectroscopy (FTIR). The infrared spectra of the samples were measured over a wavelength range of 4000-500 cm^{-1} and acquired in the spectral range through the accumulation of 8 scans with a 4 cm^{-1} .

2.9 Multilayer hydrogel

As the final stage of the present work, a multilayer hydrogel based on collagen/collagen–gelatin particles/collagen- LMWHA acting as a drug and/or cell delivery system was developed (Figure 9).

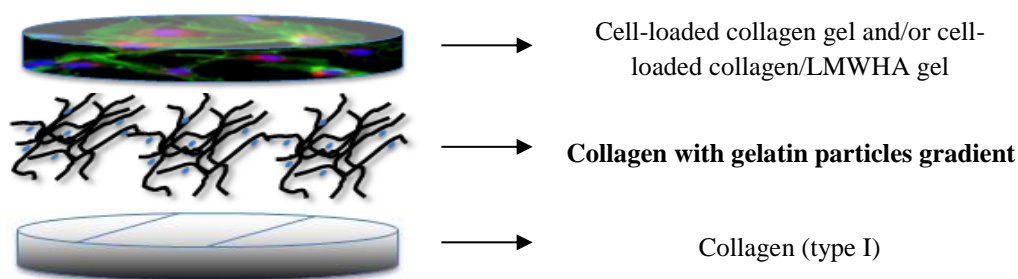


Figure 9 – Representation of the multilayer composite hydrogel with a gradient of gelatin particles.

Eight different systems were produced which are described in the following table (Table II).

	Lower	Middle	Upper
System 1	Collagen 5 mg/ml	Collagen 5 mg/ml	Collagen 1.2 mg/ml
System 2		Collagen 5 mg/ml Gelatin particles 0.025 mg/ml	
System 3		Collagen 5 mg/ml Gelatin particles 0.05 mg/ml	
System 4		Collagen 5 mg/ml Gelatin particles 0.1 mg/ml	
System 5		Collagen 5 mg/ml	

System 6		Collagen 5 mg/ml Gelatin particles 0.025 mg/ml	1.2 mg/ml +
System 7		Collagen 5 mg/ml Gelatin particles 0.05 mg/ml	LMWHA 2.5 mg/ml
System 8		Collagen 5 mg/ml Gelatin particles 0.1 mg/ml	

Table II – Composition of each single system composed by three different layers.

The viscoelastic properties as well as the morphological and biological features of the different developed systems have been studied. Rheological analyses (i.e. small amplitude oscillatory shear tests and steady state shear measurements) were performed on all the proposed systems in order to highlight its mechanical spectra.

2.10 Rheological Analysis

The mechanical properties of hydrogels have been demonstrated to be an important parameter to understand whether a hydrogel is suitable for a specific biological application. The crosslinking density of the polymers influences the mechanical properties of hydrogels and consequently the spreading behavior of cells. The cellular behavior can be improved by manipulating the stiffness of the hydrogels since the decreasing of stiffness increases the pore size and then favors cell spreading. On the other hand, mechanical properties are improved by increasing the substrate stiffness which is related to the increase of polymer concentration [101].

Among others methods, oscillatory rheometry, dynamic mechanical analysis (DMA) and elongation/compression analysis are the most commonly used. It provides information on the gel strength by terms of viscosity or elasticity and its dependence on gel composition and stability [102].

Rheology constitutes the first experimental method to assess the viscoelastic properties of hydrogels. Small amplitude oscillatory shear tests allow the evaluation of the time-dependent response and linear viscoelastic properties of hydrogels. These measurements are performed within linear viscoelastic region of a material to ensure a no dependence of the magnitude of imposed strain or stress on the measured hydrogel properties.

So, a sinusoidal shear strain is imposed to the material:

$$\gamma = \gamma_0 \sin(\omega t)$$

and the measured shear stress (τ), which is intermediate between an ideal pure elastic solid and an ideal viscous fluid for viscoelastic materials, is phase-shifted with respect to the applied deformation:

$$\tau = G'(\omega)\gamma_0 \sin(\omega t) + G''(\omega)\gamma_0 \cos(\omega t)$$

in which γ_0 is the shear strain amplitude, ω the oscillation frequency, t the time, $G'(\omega)$ the storage or elastic modulus and $G''(\omega)$ the loss or viscous modulus. The elastic modulus measures the energy stored in the material during deformation or elasticity and the viscous modulus the energy dissipated as heat during shear, the viscous component. The loss tangent or loss factor is defined as the ratio between these two moduli:

$$\tan \delta = \frac{G''}{G'}$$

where δ is the phase angle. If $\tan \delta > 1$ the material shows a viscous liquid behavior, on the contrary if $\tan \delta < 1$ it behaves as an elastic solid [103].

Hydrogels constitute an excellent approach for the development of injectable drug vehicles as long as they present accurate flow properties: shear-thinning and self-healing behavior.

Viscosity as a function of shear rate can be assessed by steady shear tests knowing that the strains during injection-based measurements are usually higher to the ones applied by oscillatory rheometer. Injection of a gel may influence its rheological behavior and viscoelastic properties. Since the materials are injected through a catheter it can disrupt the polymer network decreasing its elastic modulus and consequently its gel-like behavior. [26, 104]

2.10.1.1 Small amplitude oscillatory shear tests

Small amplitude oscillatory shear tests were carried out in order to evaluate the time-dependent response of the materials and their linear viscoelastic properties. All of the measurements were performed at a temperature of 37°C, using a rheometer (Gemini, Bohlin, Sweden). The frequency was varied from 0.1 to 10 Hz. The dynamic moduli G' (storage modulus or elastic modulus) and G'' (loss modulus or viscous modulus) were evaluated in the frequency range investigated as follows:

$$G' = \frac{\tau_0}{\gamma_0} \cos \delta$$
$$G'' = \frac{\tau_0}{\gamma_0} \sin \delta$$

where δ is the phase shift between the input and the output signals (the stress, τ , and the strain, γ , respectively), whilst τ_0 and γ_0 represent stress and strain amplitudes.

2.10.1.2 Steady shear measurements

The viscosity as a function of the shear rate was evaluated through steady state shear measurements performed on the proposed materials. All the measurements were carried out at a temperature of 37°C in a wide range of shear rate (0.01 – 100 s⁻¹), using a rheometer (Gemini, Bohlin, Sweden).

2.11 Injectability tests

The injectability of collagen gels and collagen-LMW HA s-IPNs was investigated by means of an INSTRON 5566 testing machine, using a custom-made experimental setup schematically reported in Figure 10.

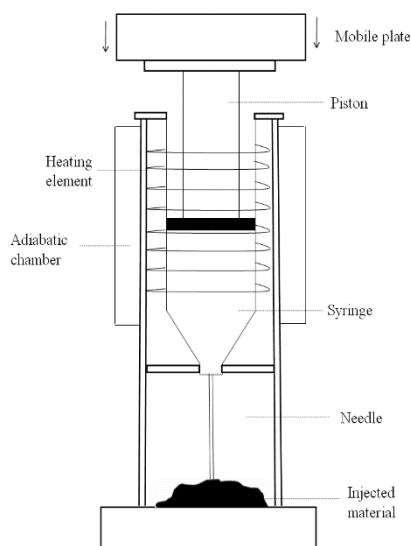


Figure 10 – Schematic representation of the experimental setup used to carry out the injectability tests.

The injectability measurements were performed using a syringe with a 26 G needle. The syringe (with an inner diameter of 4.5 mm) was filled with the material which was then injected through the needle by applying a force on the syringe piston. This device was mounted on the INSTRON 5566 testing machine and the piston was driven at a constant and a fixed speed of 40 mm/min, thus controlling the injection rate and the apparent shear rate in the needle. All the tests were carried out at 37°C. The load applied to the piston for injecting the material into and through the 26 G needle was measured using a suitably calibrated load cell. An empty syringe (with a 26 G needle) was also tested at the same speed to estimate the effect due to the friction between syringe wall and piston.

2.12 Cell adhesion study

Human mesenchymal stem cells (hMSCs - Clonetics, Italy), at the 4th passage, were cultured in α -Modified Eagle's medium (α -MEM) containing 10% (v/v) FBS, 100 U/ml penicillin and 0.1 mg/ml streptomycin, in a humidified atmosphere at 37°C and 5% CO₂. Preliminary results were obtained suspending 8×10^5 hMSCs in 1 mL of collagen 1.2 mg/ml and collagen/hyaluronic acid 2.5 mg/ml. Cell constructs were placed in 24 well culture plates and, incubated for 30 minutes in a humidified atmosphere (37°C, 5% CO₂) to promote collagen fibrillogenesis. Subsequently, 0.5 ml of cell-culture medium was added to each well. The gels were maintained in culture for 5 days and the cell-culture medium was changed after 2 days. Cultures were characterized in terms of cell attachment and proliferation and preliminary results on cell morphology were obtained by means of a photcamera-equipped optical microscope. Cell viability and proliferation were evaluated by using the MTT assay (reduction of 3-(4, 5-dimethylthiazol-2-yl)-2,5-diphenyltetrazolium bromide to a purple formazan product). The cell-matrix medium was removed from the culture plates at days 2 and 5, washed with PBS (Sigma-Aldrich, Italy), and placed into 24 well culture plates. For each gel, 1 ml of DMEM medium without Phenol Red containing 10% (v/v) MTT assay was added, followed by incubation for 4 h at 37°C and 5% CO₂. The solution was subsequently removed from the wells and analyzed by a spectrophotometer at 570 nm. The number of viable cells into the gels was finally determined by comparing the absorbance values at different culture times with those of the calibration curve. The calibration curve was obtained from the correlation between known cell numbers in the 24 well culture plates with the corresponding absorbance values. Results are presented as mean \pm standard deviation in triplicate.

Considering the optimized multilayer hydrogel, human mesenchymal stem cells were statically seeded and grown in Dulbecco's modified Eagle's medium (DMEM) without fetal bovine serum (FBS).

In order to evaluate cell adhesion and viability/proliferation, the Alamar Blue assay (AbD Serotec Ltd, UK) was also performed on the 3D cell constructs (hMSC-multilayer hydrogel). Alamar Blue assay was also used for the evaluation of cytocompatibility of gelatin particles alone or embedded into the collagen matrix.

The Alamar Blue Assay is based on a redox reaction that occurs in the mitochondria of the cells. Thus, the colored product is transported out of the cell and can be measured through a spectrophotometer. Specifically, at 1, 3 and 7 days after cell seeding, the cell constructs were rinsed with PBS (Sigma-Aldrich, Italy), and for each sample, 200 ml of DMEM without Phenol Red (HyClone, UK) containing 10% (v/v) Alamar Blue (AbD Serotec Ltd, UK) was added, followed by incubation in 5% CO₂ diluted atmosphere for 4 h at 37°C. A specific volumetric amount of solution was then removed from the wells and transferred to a new 96-well plate. The optical density was immediately measured with a spectrophotometer (Sunrise; Tecan, Männedorf, Zurich, Switzerland) at wavelengths of 570 and 595 nm [105]. The number of viable cells correlates with the magnitude of dye reduction and is expressed as a percentage of Alamar Blue reduction, according to the manufacturer's protocol. Each experiment was performed at least three times. Cell densities of 1.5×10^4 and 3×10^4 cells per sample were used for cell adhesion and viability/proliferation tests, respectively. The cell-particle interactions as well as the different kinds of cell constructs were analyzed at different times after cell seeding using confocal laser scanning microscopy (CLSM). Cell constructs were fixed with 4% paraformaldehyde for 20 min at room temperature, rinsed twice with PBS buffer and incubated with PBS-BSA 0.5% to block unspecific binding. Actin microfilaments were

stained with phalloidin tetramethylrhodamine B isothiocyanate (Sigma-Aldrich). Phalloidin was diluted in PBS-BSA 0.5% and incubated for 30 min at room temperature. The images were acquired at different times from cell seeding by using a He-Ne excitation laser at the wavelength of 543 nm and a 20x objective.

Image J software (National Institutes of Health, USA) was involved for quantitatively evaluation of the cell morphology using a shape factor. The shape factor was expressed as follows:

$$\Phi = \frac{\Theta A}{P^2}$$

where Θ represents a geometric constant (4π) related with the footprint area A and P is the perimeter of a cell [106].

Alamar blue assay has been also performed in order to evidence results in terms of Human Umbilical Vein Endothelial Cells (HUVECs) adhesion and viability/proliferation on the cell constructs at different culture times, also evidencing the effect of the inclusion of VEGF-loaded GPs and PlGF-loaded GPs on cell behaviour, over time. HUVECs (HUVEC – Clonetics, Italy) were prepared and analyzed as reported in the literature [107]. Briefly, they were grown in human endothelial-SFM basal growth medium supplemented with HI-FBS, 1% endothelial cell growth factor (ECGS), 100U/ml porcine heparin, 1% pen/strep in a humidified atmosphere at 37°C and 5% CO₂, and used at early passages (I–IV).

HUVECs were statically seeded on the optimized multilayer composite hydrogel, collagen (1.2 mg/mL), collagen-LMWHA (1.2 mg/mL – 2.5 mg/mL), collagen (1.2 mg/mL) reinforced with GPs.

GPs were loaded with VEGF (25 ng/mL) and PlGF (10 ng/mL), and the effects on cell behavior were investigated. In order to evaluate cell adhesion and viability/proliferation, the Alamar Blue assay (AbD Serotec Ltd, UK) was also performed on the different 3D cell constructs (HUVEC- hydrogel). Specifically, at 1, 3 and 7 days after cell seeding, the optical density was measured with a spectrophotometer (Sunrise; Tecan, Männedorf, Zurich, Switzerland) at wavelengths of 570 and 595 nm [105]. 8×10^4 cells per sample were used for cell adhesion and viability/proliferation tests.

The several kinds of cell constructs were also analyzed at different times after cell seeding using optical microscopy. In vitro methods suitable for drug validation and for quantifying angiogenesis (i.e., Matrigel Assay) were also considered.

3 Results and Discussion

3.1 Small amplitude oscillatory shear tests

Small amplitude oscillatory shear tests have shown a gel-like behaviour for all the proposed materials, as the storage modulus G' is always greater than the loss modulus G'' in the frequency range investigated (Figure 11). Both dynamic moduli depend on frequency and collagen - LMW HA composition, generally rising with frequency and collagen concentration.

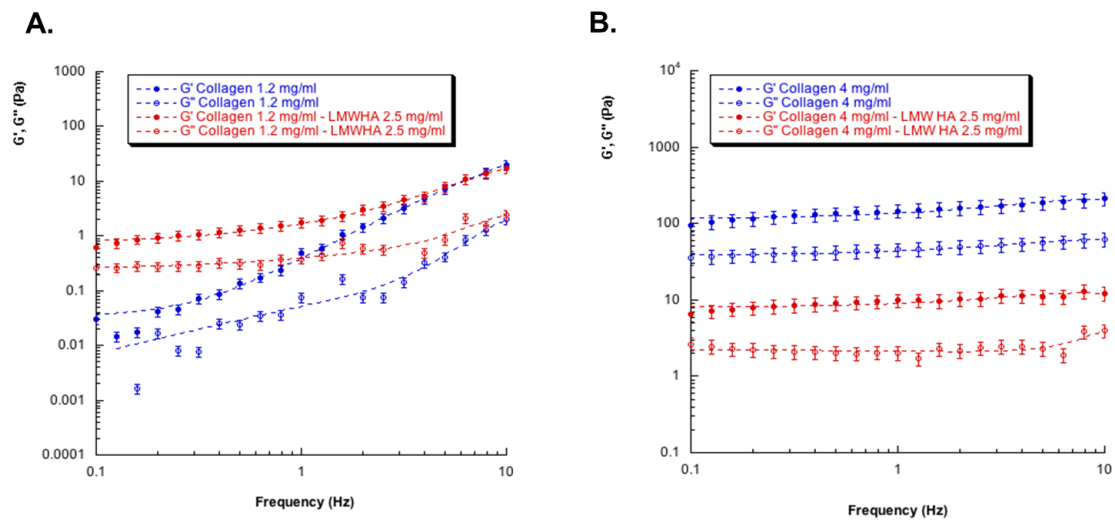


Figure 11 – Mechanical spectra of: A. Collagen 1.2 mg/ml and collagen 1.2 mg/mL – LMW HA 2.5 mg/mL; B. collagen 4 mg/ml and collagen 4 mg/mL – LMW HA 2.5 mg/mL.

Values of dynamic moduli G' and G'' increased by increasing collagen concentration.

3.2 Steady shear measurements

Steady state shear measurements performed on all the materials have shown a shear thinning behaviour: viscosity decreases as the shear rate increases (Figure 12). This behaviour clearly suggests the possibility to inject the materials.

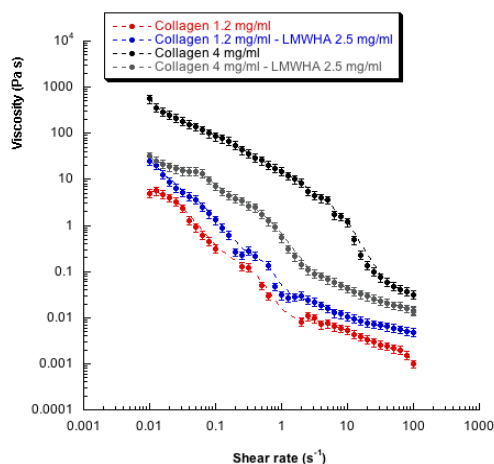


Figure 12 – Viscosity as function of shear rate for selected collagen-based materials: collagen 1.2 mg/ml and collagen 1.2 mg/ml- LMW HA 2.5 mg/ml; collagen 4 mg/ml and collagen 4 mg/ml – LMW HA 2.5 mg/ml.

3.3 Injectability tests

The injectability of collagen gels and collagen-LMW HA s-IPNs has been evaluated from the load-displacement curves, using the experimental setup schematically reported in Figure 10. The above-mentioned materials have generally shown similar load-displacement curves: a linear region is initially observed at low displacement values. After a maximum load occurred, load values sharply dropped, then fluctuating and reaching a plateau. At the end of the plateau-like region all the materials were completely injected (Figure 13).

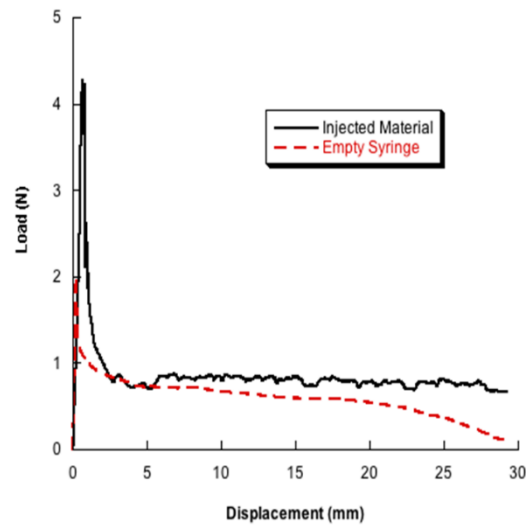


Figure 13 - Typical load-displacement curve obtained from a material injected into and through the 26 G needle (solid line) in comparison with an empty syringe (dashed line).

Mean values of maximum load and plateau load have been reported in the following table (Table III).

Material	Maximum Load (N)	Plateau Load (N)
Empty Syringe	2.07 ± 0.31	0.65 ± 0.13
Collagen (1.2 mg/ml)	3.48 ± 0.70	1.33 ± 0.31
Collagen (1.2 mg/ml) – LMW HA (2.5 mg/ml)	3.58 ± 0.45	1.17 ± 0.19
Collagen 4 mg/ml	4.11 ± 0.45	1.58 ± 0.11
Collagen (4 mg/ml) – LMW HA (2.5 mg/ml)	4.31 ± 0.44	1.49 ± 0.41

Table III - Results obtained from the injectability tests. Maximum load and plateau load reported as mean value \pm standard deviation.

As already discussed, it appears clear that the values of maximum load also include the contribution of the initial friction. For this reason, the maximum load may represent the initial resistance to material flow, whilst the plateau load may give important information on the continuous flow of material through the needle.

3.4 Gelatin particles

The preparation of biodegradable gelatin particles (GPs) was accomplished by the optimized conditions of the two-step desolvation method. Figure 14A shows the micrograph of the obtained gelatin particles without BSA, revealing a uniform spherical shape with a smooth surface.

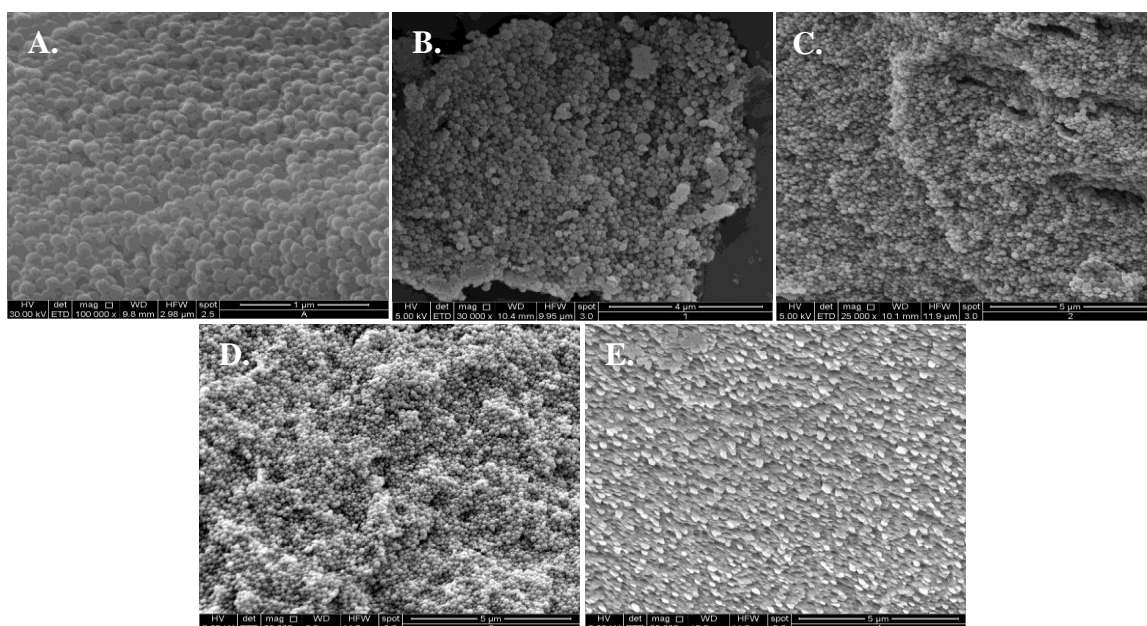


Figure 14 - SEM micrographs showing the morphology of gelatin particles with different BSA loadings (w/w): A. 0% B. 0.2% C. 0.5% D. 1% E. 2%.

BSA, a model protein, is normally used in various studies due to its abundance and low cost. In this study, before using the desired protein, the varying BSA loading was tested for its effect on the morphology of the particles (Figure 14B-E). There were no differences on the morphology when BSA was added (Figure 14B-D), except for 2% w/w BSA where seems to occur an elongation of the particles showing a non-spherical geometry and roughness on the surface (Figure 14E).

When designing drug delivery systems, size plays an important role since it influences the drug release rate. Figure 15 shows the influence of BSA loading on particle size. The results showed that the encapsulation process affects the gelatin particles as the particle size seems to decrease by increasing the amount of BSA. The average mean size for the

unmodified gelatin particles was 195 nm and about 150 nm for 1% w/w BSA. However, there are no significant differences in particle size among the produced gelatin particles.

Particle size prior to lyophilisation was also evaluated by laser diffractometry. As discussed before, the results showed an influence of the encapsulation process and the results showed a unimodal distribution, with a low PDI.

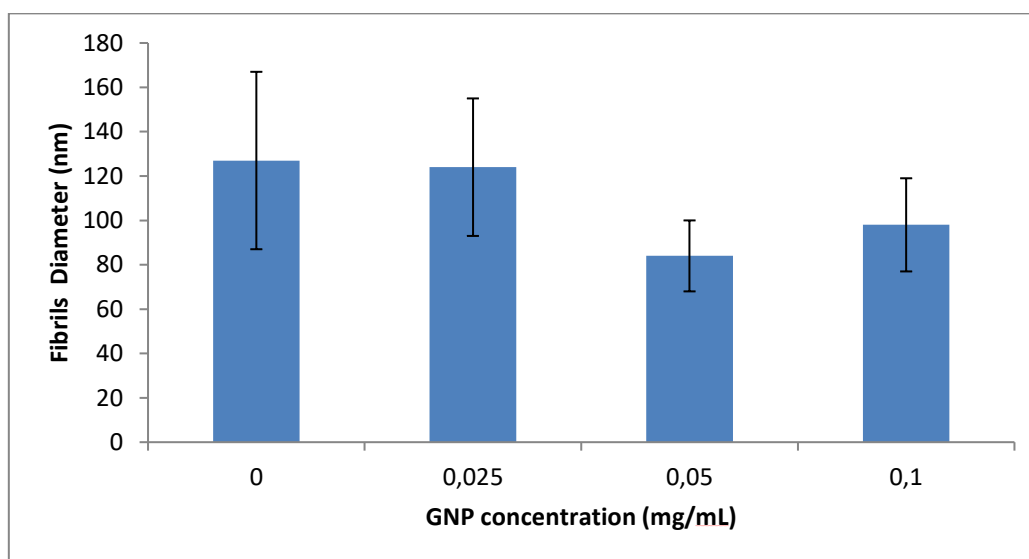


Figure 15 - Variation of fibrils diameter with the concentration of gelatin particles.

The matrix morphology of dried collagen hydrogels and collagen-GPs samples were examined by SEM at different magnifications (Figure 16). For the collagen hydrogel, a fibrillar and highly porous structure with macropores and smaller interconnecting pores was obtained (Figure 16A). This feature is very important because it allows cells, embedded in the scaffold, to properly adhere and proliferate. Moreover, the presence of interconnecting pores makes possible a good distribution of the nutrients which may reach all the cells and also the residues do not stay confined to a single pore thus compromising cell survival. The middle layer was prepared by mixing homogeneously the GPs at various concentrations with the collagen solution. Then, the final solution was electro sprayed on the collagen hydrogel prepared previously (lower layer). For the collagen-

gelatin particles hydrogels, SEM analysis showed also a highly fibrillar collagen structure (average diameter size of 100 nm) where gelatin particles with similar size (60 nm) were embedded and well-integrated in the collagen network (Figure 16B).

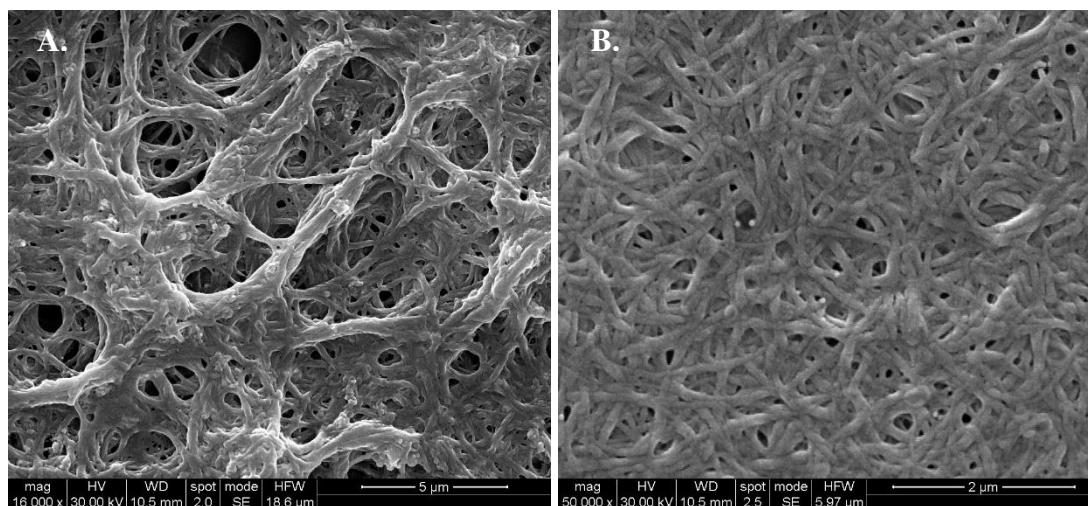


Figure 16 – SEM images of the dried hydrogels at different magnifications. A. Collagen hydrogel 5 mg/mL and B. Collagen-GPs (0.05mg/mL) hydrogel.

3.5 Cumulative release of BSA from gelatin particles

The release profiles of BSA from the systems were also measured by UV-Vis spectrophotometer (Perkin Elmer), evaluating the absorbance at a wavelength of 278 nm. Figure 17 shows typical release profiles. At the initial stage a fast release phase is evident, then followed by a slower phase.

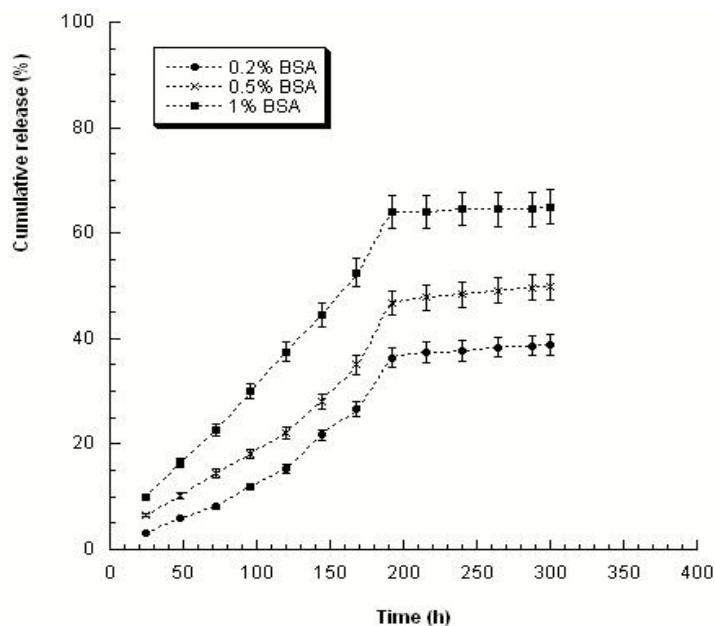


Figure 17 – Cumulative release over time.

3.6 Solid phase peptide synthesis (SPSS) and functionalization of gelatin particles

Solid phase peptide synthesis has demonstrated to be an adequate method to produce complex sequences such as FFG3K. Mass spectrum shows a main peak corresponding to the desired product (Figure 18).

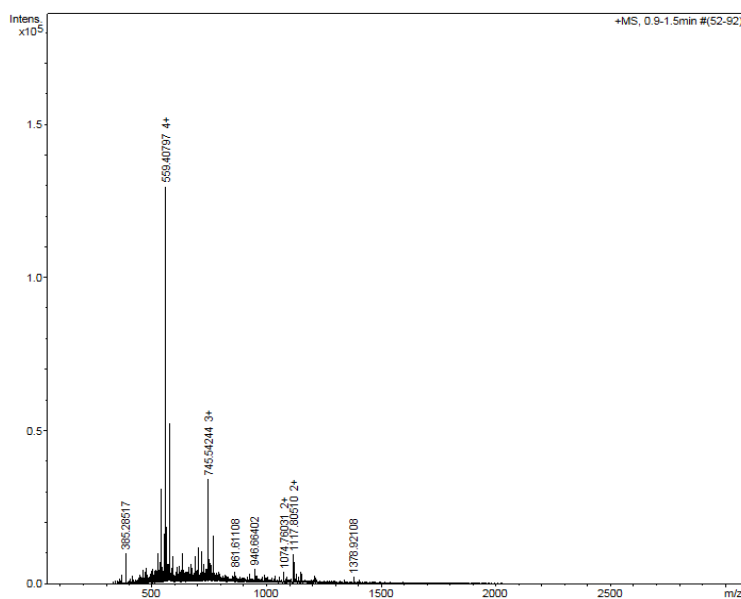


Figure 18 - Mass spectrum of FFG3K.

This value corresponds to a fourfold charged ion with a total molecular weight of 2237.63 and is in accordance with the theoretical one of FFG3K 2234.95. Minor peaks might be attributed to the system noise or some fragments of the sequence. GPs were functionalised with FFG3K by the EDC/NHS coupling reaction. Functionalised GPs were characterised by attenuated reflectance Fourier transform spectroscopy (FTIR). The infrared spectra of the samples were measured over a wavelength range of 4000-500 cm^{-1} and acquired in the spectral range through the accumulation of 8 scans with a 4 cm^{-1} . Specifically, FTIR was performed on GPs, FFG3K and 10% and 20% of total functionalisation of the GP to determine whether the process of functionalization was well succeed (Figure 19). GPs show the typical peaks of the raw gelatin. An amide I peak (C=O stretch) at 1620-1635 cm^{-1} , amide II peak (N-H bend and C-H stretch) at 1520-1540 cm^{-1} , amide III peak (C-N stretch and N-H in phase bending) at 1240 cm^{-1} and amide A peak (N-H stretching vibration) at 3300 cm^{-1} . In the functionalised GPs, all these peaks were present but most of them much stronger and shifted. Furthermore, additional peaks were also formed such as the peak at 1200 cm^{-1} where it changed from smooth to two peaks.

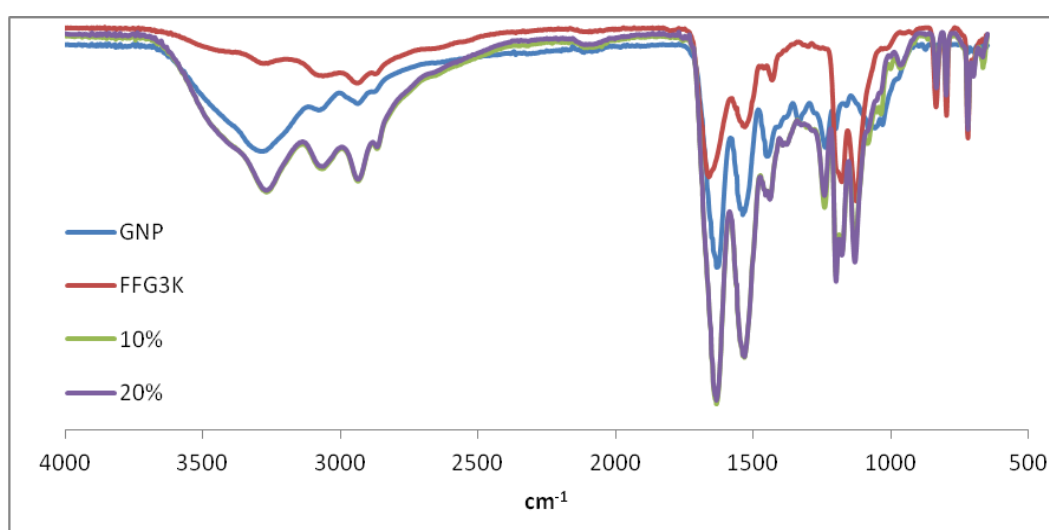


Figure 19 - FTIR of GPs, FFG3K and GPs functionalized with FFG3K (10% and 20% of total functionalization).

3.7 Multilayer hydrogels

For all the analyzed systems, a gel-like behavior was also observed (Figure 20). Both dynamic moduli increased with the frequency. As for the systems with the LMWHA-based middle layer (systems 5-8 described in 2.9) both G' and G'' values increased with GP concentration, thus acting as a reinforcement for the system up to a threshold concentration.

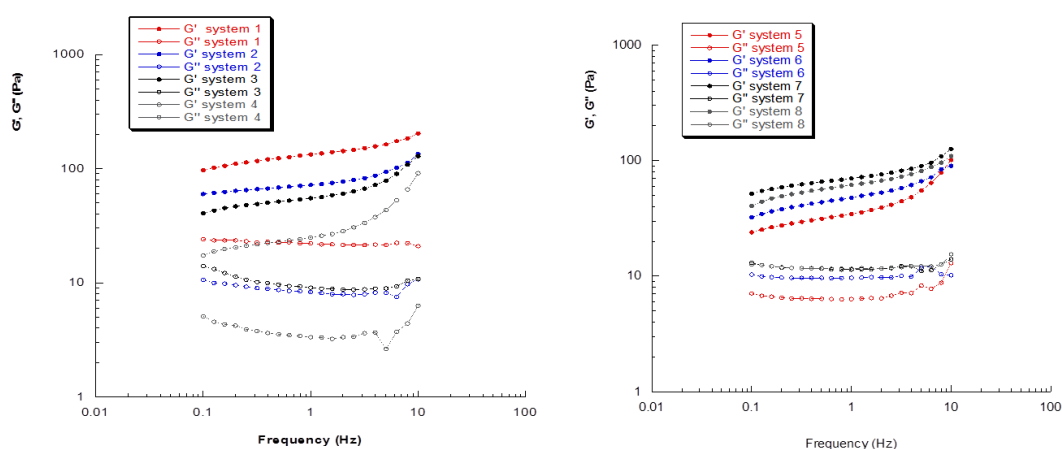


Figure 20 - Mechanical spectra for all the systems depicted in 2.9.

When in the presence of hMSCs, at day 0, the gel like behavior was not altered. However, by increasing the amount of gelatin particles systems on the systems composed by LMWHA, both G' and G'' values decreased (Figure 21). This behavior might change over time by the production of ECM, which makes the system more rigid, thus increasing both dynamic moduli.

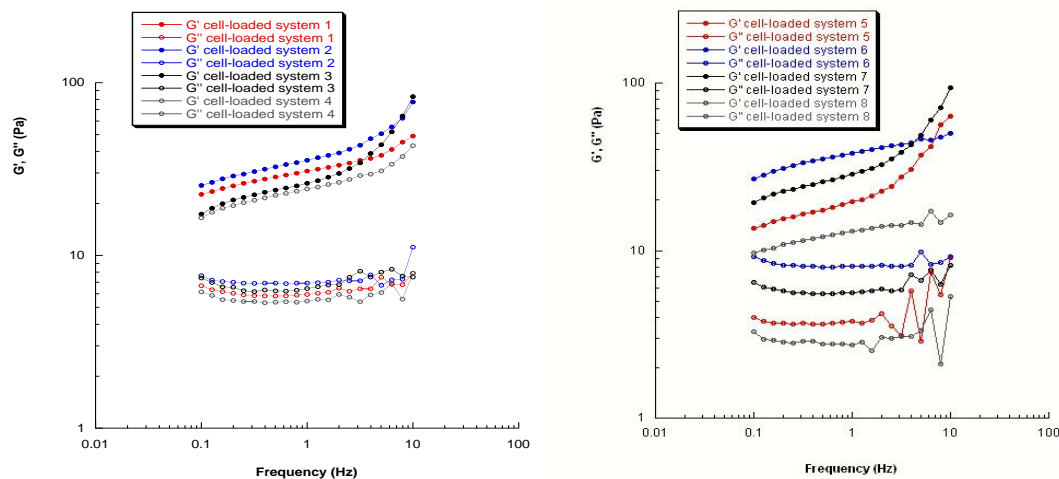


Figure 21 - Mechanical spectra for all cell-loaded multilayer composite hydrogels at day 0.

For all the analyzed systems, mechanical spectra with G' values higher than G'' ones were observed. Both dynamic moduli increased with the frequency. It is well known that the inclusion of particles influences both dynamic moduli and G' values generally increase with particle concentration [26, 105]. However, after the injection through clinical needles, G' decreases when the particle concentration is increased beyond a threshold limit. In particular, if the particle concentration exceeds a threshold value, the polymer-based network can be completely destroyed during the injection through clinical needles, as the particles start to act as “weak points” for the system as already reported in the literature [26, 108].

3.8 Cell adhesion study

Interesting results in terms of cell adhesion and viability/proliferation tests were obtained. HMSC viability was assessed for all the proposed systems and the presence of collagen/LMWHA-based materials seems to favor cell attachment and spreading. The following Figure 22 summarizes the results obtained from MTT assay and imaging microscopy in terms of cell viability and attachment over time.

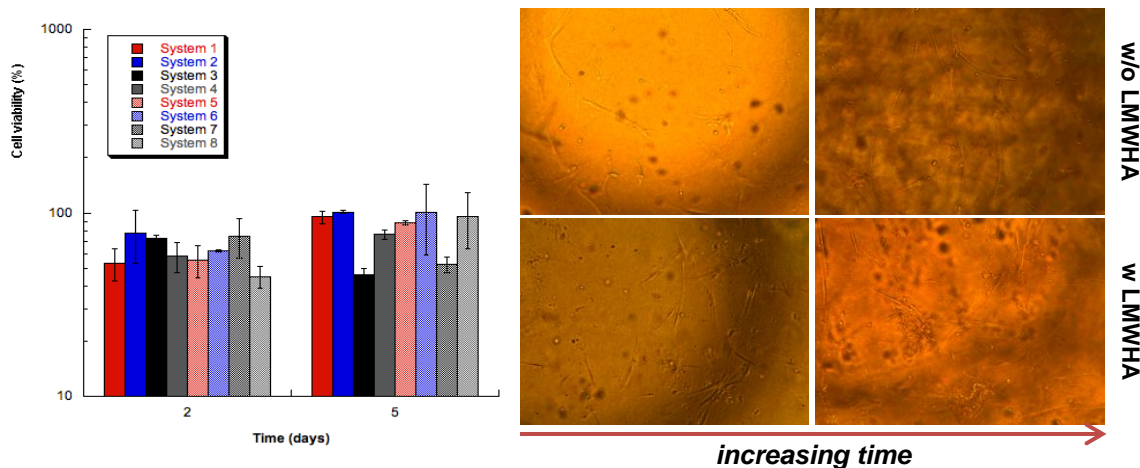


Figure 22 – MTT assay and imaging microscopy.

Thus, taking into account the rheological/mechanical results, as well as the structural/functional features, the multilayer hydrogel marked as “system 6” was selected for further analysis.

Alamar blue assay performed on cell constructs characterized by collagen-LMWHA gels with BSA-loaded gelatin particles have highlighted that hMSCs are viable on all the proposed materials. There was no significant difference in cell adhesion with varying BSA concentration after 1 day (Figure 23). Cell viability was significantly higher after 7 days with a 1% BSA concentration (Figure 24).

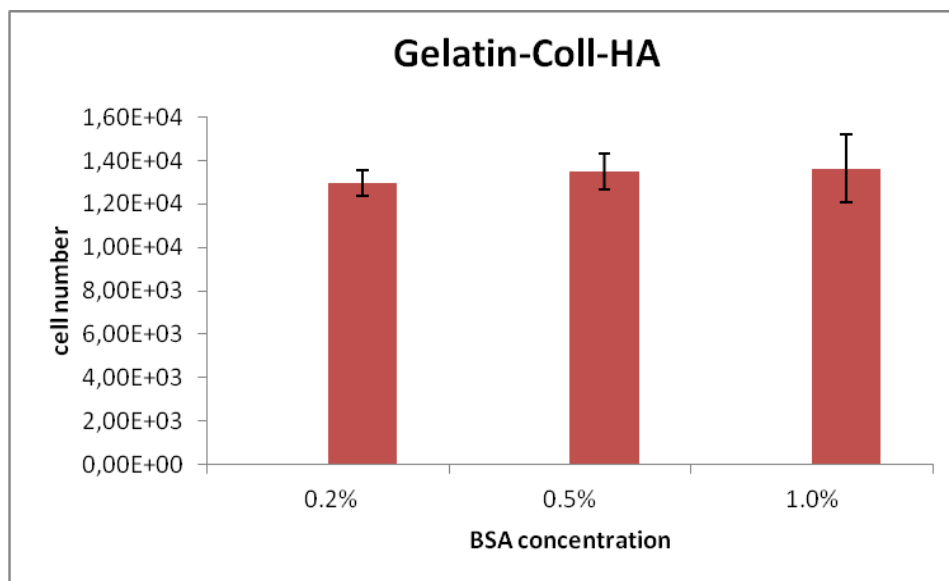


Figure 23 - Alamar Blue assay: adhesion tests and effects of BSA-loaded particles embedded in the matrix. GPs were loaded with different BSA concentrations (0.2, 0.5, and 1%).

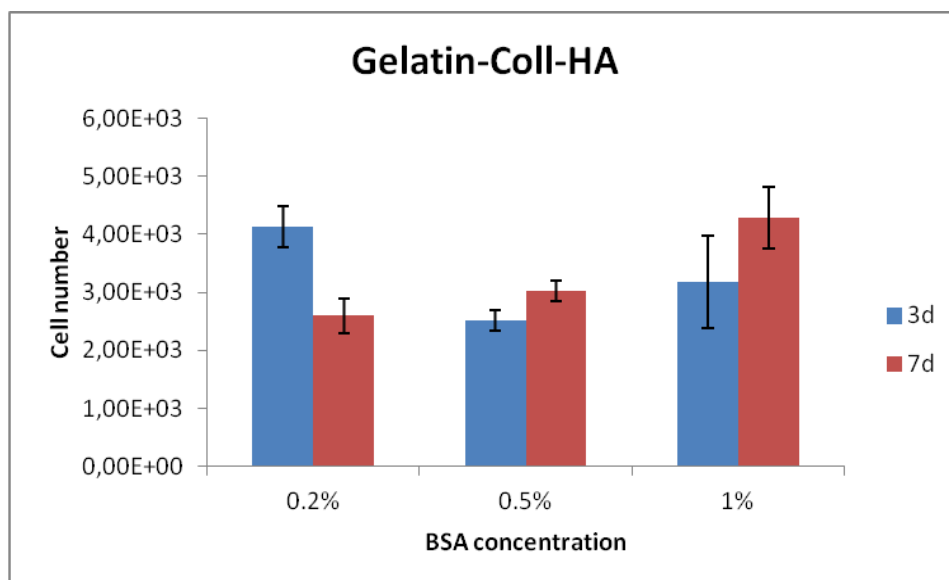


Figure 24 - Alamar Blue assay: viability/proliferation tests and effects of BSA-loaded particles embedded in the matrix. GPs were loaded with different BSA concentrations (0.2, 0.5, 1%)

On the other hand, CLSM images obtained from cell-particle interactions and from all the 3D cell constructs (hMSC-multilayer hydrogel) (Figure 25 and Figure 26) were also suitably analysed through Image J software (National Institutes of Health, USA) to evaluate the cell morphology using a shape factor. The shape factor was expressed as follows:

$$\Phi = \frac{\Theta A}{P^2}$$

where Θ represents a geometric constant (4π) related with the footprint area A and P is the perimeter of a cell [106].

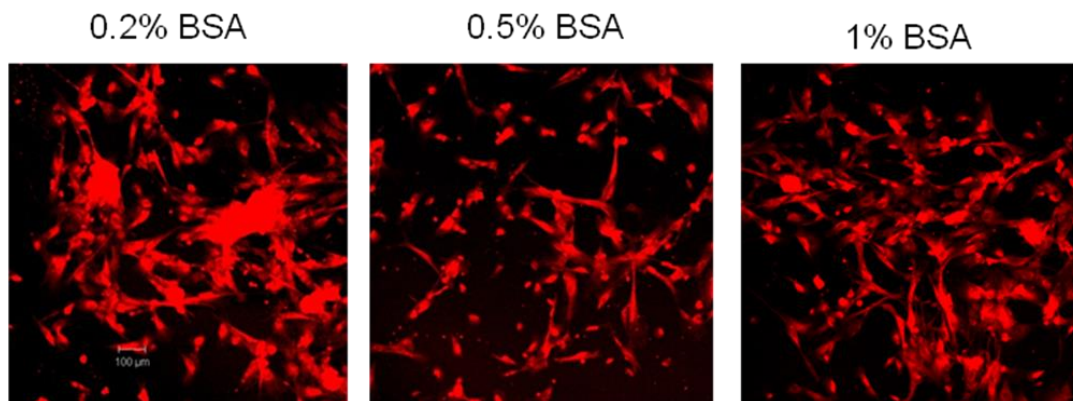


Figure 25 - Results from CLSM analysis on cell-particle interactions at 7 days after cell seeding.

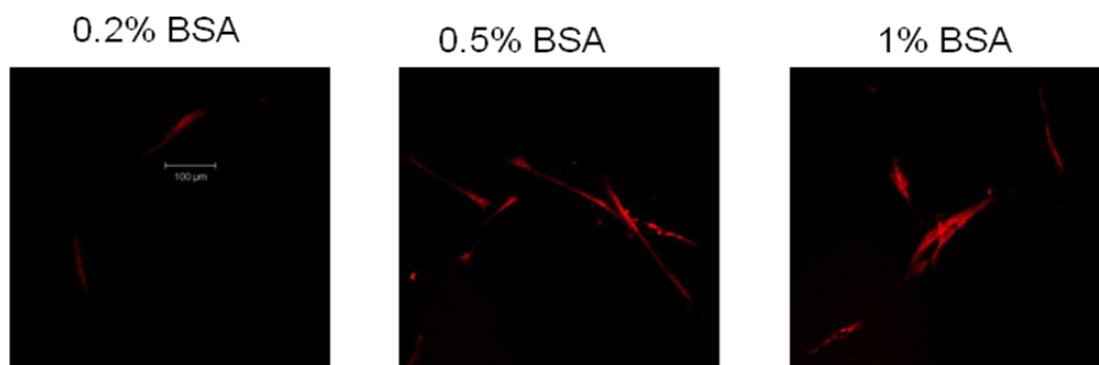


Figure 26 - Results from CLSM analysis on 3D cell constructs at 7 days after cell seeding.

Considering that circular objects possess the greatest area-to-perimeter ratio, a shape factor of 1 represents a perfect circle. On the other hand, a thin thread-like object has the lowest shape factor approaching zero. Thus, studies on cell adhesion and spreading were also performed based on CLSM images, the aim being to determine the shape factor of the cells. As an example, for the optimised system with BSA (1%)-loaded particles, the cell shape factor decreased significantly from 0.79 ± 0.04 at day 1 to 0.09 ± 0.01 at day 7. It is worth noting that the lower the cell shape factor, the more elongated the cells [108].

Briefly, an increased total cellular area (i.e., the establishment of multiple cellular extensions) implies elongated cells and, hence, the reduction in the shape factor, thus leading to better adhesion and spreading process.

Figure 27 reports the results in terms of cell adhesion and viability/proliferation obtained by the Alamar Blue assay performed on the cell constructs at different culture times, in the presence of VEGF- and PlGF-loaded gelatin particles. In comparison to the neat collagen, cell adhesion was better on collagen with VEGF- and PlGF-loaded GPs. However, in terms of cell adhesion, at day 1 there were no significant differences between collagen with VEGF-loaded GPs and collagen with PlGF-loaded GPs. At day 3, in terms of cell proliferation, differences were found between collagen with VEGF-loaded GPs and collagen with PlGF-loaded GPs. The effect of PlGF was evident over 3 days and then decreased until day 7. On the other hand, the effect of VEGF decreased after 1 day. All of these results were also consistent with those obtained from optical imaging microscopy.

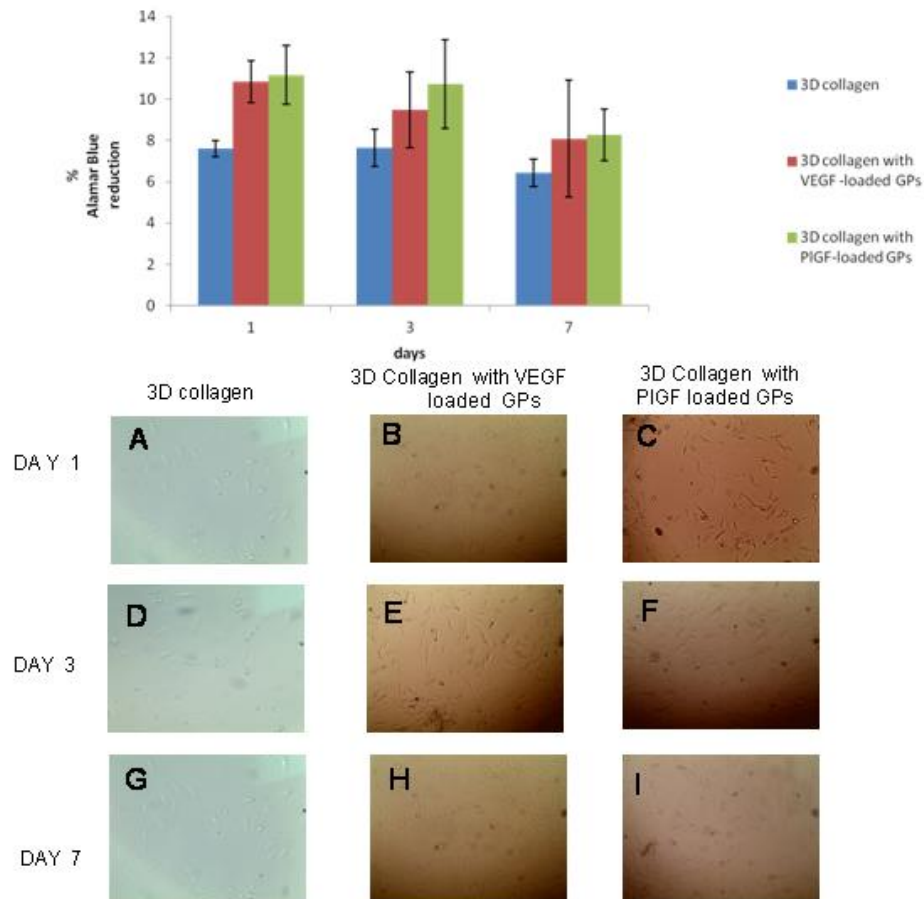


Figure 27 - Alamar Blue assay: HUVEC adhesion and proliferation in collagen and collagen reinforced with GPs. In panels A–I are reported representative microscopy images of HUVEC culture at day 1, 3 and 7: collagen (A, D, G); collagen with VEGF-loaded GPs (B,E,H); collagen with PIGF-loaded GPs (C,F,I).

Figure 28 reports the results in terms of cell adhesion and viability/proliferation obtained by the Alamar Blue assay performed on the cell constructs at different culture times. If compared to the neat collagen-LMWHA, cell adhesion (i.e., at day 1) was better on the optimized systems with VEGF- and PIGF-loaded GPs. However, differently from collagen with VEGF-loaded GPs, in the multilayer systems with VEGF-loaded GPs a slight decrease of cell proliferation was observed at day 7 consistently with the results from optical microscopy. Differently from the systems reinforced with VEGF-loaded GPs, cell proliferation increased over time for the multilayer systems with PIGF-loaded GPs.

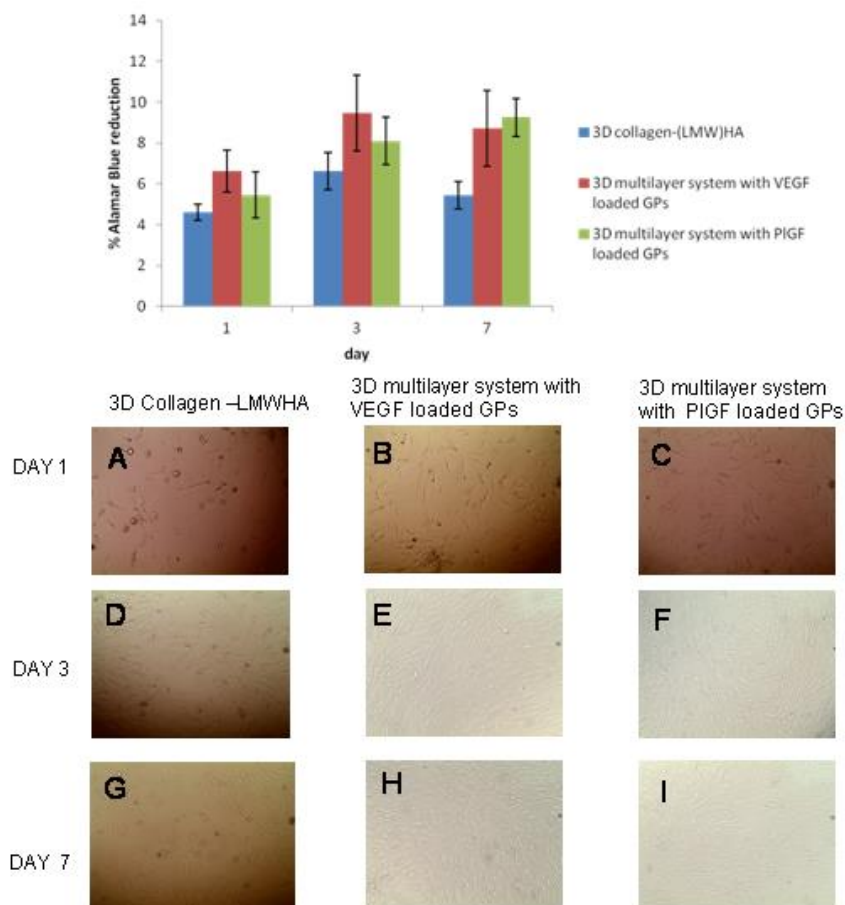
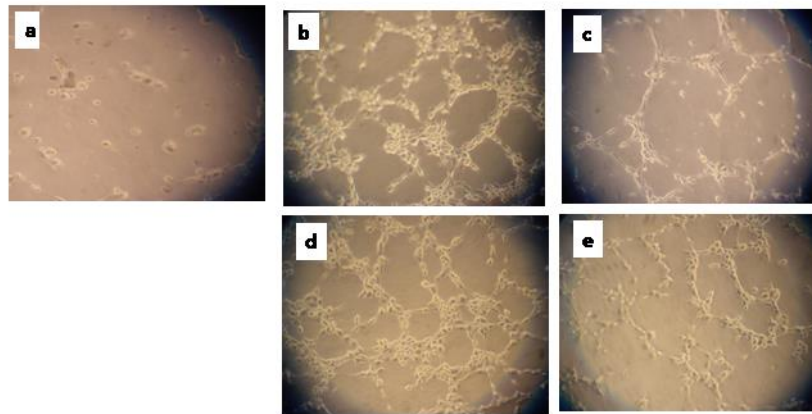


Figure 28 - Alamar Blue assay: HUVEC adhesion and proliferation in collagen-LMWHA and multilayer systems with GPs. In panels A–I are reported representative microscopy images of HUVEC culture at day 1, 3 and 7: collagen-LMWHA (A, D, G); multilayer system with VEGF-loaded GPs (B,E,H); multilayer system with PIGF-loaded GPs (C, F, I).

The bioactivity of the VEGF released from GPs after 6 h was evaluated by an in vitro bi-dimensional tube formation assay (Figure 29). This assay was chosen since it is one of the most widely used test for the evaluation of the efficacy of pro-angiogenic factors in vitro. As evidenced by preliminary experiments, VEGF-loaded GPs showed no cytotoxicity effect on HUVECs when cultured in the presence of either a GP-preconditioned medium or a medium with GPs (data not shown). Then, HUVECs were plated onto a Matrigel coat and the angiogenic response was measured by the extent and shape of the capillary-like network formed by HUVECs after 6 h of incubation in culture medium without angiogenic inducer (Figure 29A), with free VEGF (Figure 29B) with

free PIGF (Figure 29C), with VEGF-loaded GPs (Figure 29D), with PIGF-loaded GPs (Figure 29E). It is worth noticing that in terms of number of tube-like structures and grid intersections, which were measured and quantified by Scion Image Software, no differences were found between the PIGF released from GPs and the same amount of free PIGF. Conversely, a lower number was evaluated for the VEGF-loaded GPs in comparison to that obtained for free VEGF. These results also suggested the different ability of the system to control the release of VEGF and PLGF. Furthermore, all the obtained results indicated that the process of encapsulation did not affect negatively the VEGF and PIGF biological activity.

Capillary like tube formation (Matrigel assay)

- a: HUVECs on matrigel (without FBS)
- b: HUVECs on matrigel with VEGF
- c: HUVECs on matrigel with VEGF loaded GPs
- d: HUVECs on matrigel with PlGF
- e: HUVECs on matrigel with PlGF loaded GPs

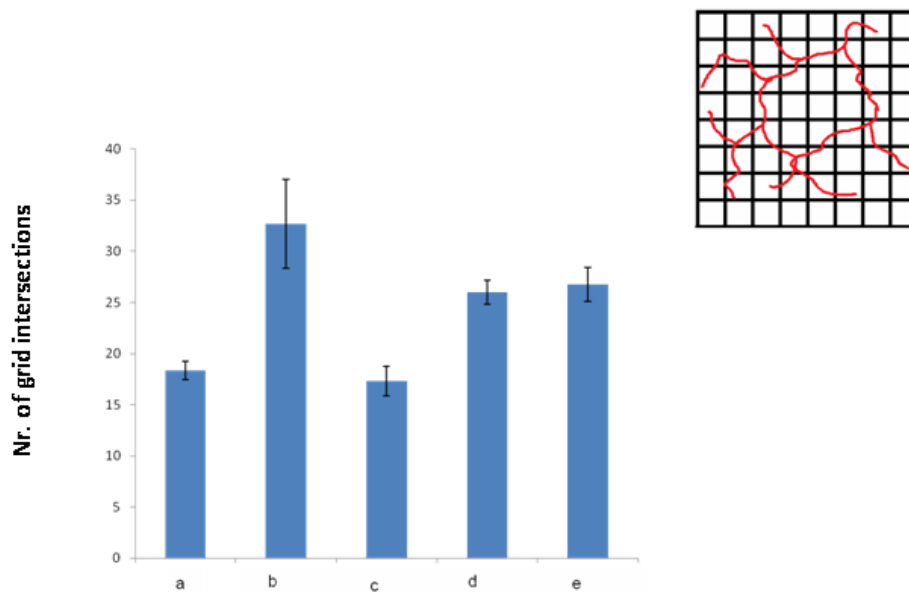


Figure 29 - Matrigel assay: capillary like tube formation and quantification of tubular structures (average number of intersections \pm SD, Scion Image Software Analysis).

4 Conclusions

A multifunctional hydrogel acting as a reservoir system to deliver specific biomolecules to targeted ischemic sites was designed in the form of a multilayer composite hydrogel integrating conventional and advanced methods (i.e., electrospray-based technique).

Protocols for scale-up of hydrogel system components were developed. Gelatin particles were further developed, loaded with a model protein (BSA) and analyzed. Gelatin particles were functionalized. Gelatin particles were also loaded with VEGF and PlGF and analyzed. The effects of the VEGF and PlGF released from GPs/multilayer system on the cell behavior, as well as the capillary like tube formation by HUVECs, were properly measured.

The optimized system was properly selected taking into account the rheological/mechanical results, as well as the structural/functional features. The developed system showed adequate mechanical/rheological properties and can be also easily injected. The biological features of the system were analyzed and the profile release was evaluated.

5 References

1. Perk, J., et al., *European Guidelines on cardiovascular disease prevention in clinical practice (version 2012)*. International Journal of Behavioral Medicine, 2012. **19**(4): p. 403-488.
2. Labarthe, D., et al., *The Public Health Action Plan to Prevent Heart Disease and Stroke: Ten-Year Update*. 2014.
3. Kim, A.S. and S.C. Johnston, *Global variation in the relative burden of stroke and ischemic heart disease*. Circulation, 2011. **124**(3): p. 314-323.
4. Sutton, M.G.S.J. and N. Sharpe, *Left ventricular remodeling after myocardial infarction pathophysiology and therapy*. Circulation, 2000. **101**(25): p. 2981-2988.
5. Creager, M.A., J.A. Kaufman, and M.S. Conte, *Acute limb ischemia*. New England Journal of Medicine, 2012. **366**(23): p. 2198-2206.
6. Mitsos, S., et al., *Therapeutic angiogenesis for myocardial ischemia revisited: basic biological concepts and focus on latest clinical trials*. Angiogenesis, 2012. **15**(1): p. 1-22.
7. Briquez, P.S., et al., *Design principles for therapeutic angiogenic materials*. Nature Reviews Materials, 2016. **1**: p. 15006.
8. Simons, M., *Angiogenesis where do we stand now?* Circulation, 2005. **111**(12): p. 1556-1566.
9. Rufaihah, A.J. and D. Seliktar, *Hydrogels for therapeutic cardiovascular angiogenesis*. Advanced drug delivery reviews, 2016. **96**: p. 31-39.
10. Patan, S., *Vasculogenesis and angiogenesis as mechanisms of vascular network formation, growth and remodeling*. Journal of Neuro-oncology, 2000. **50**(1-2): p. 1-15.

11. Naderi, H., M.M. Matin, and A.R. Bahrami, *Review Article: Critical issues in tissue engineering: biomaterials, cell sources, angiogenesis, and drug delivery systems*. Journal of biomaterials applications, 2011: p. 0885328211408946.
12. Hirschi, K.K., et al., *Vascular assembly in natural and engineered tissues*. Annals of the New York Academy of Sciences, 2002. **961**(1): p. 223-242.
13. Novosel, E.C., C. Kleinhans, and P.J. Kluger, *Vascularization is the key challenge in tissue engineering*. Advanced drug delivery reviews, 2011. **63**(4): p. 300-311.
14. Rouwkema, J., N.C. Rivron, and C.A. van Blitterswijk, *Vascularization in tissue engineering*. Trends in biotechnology, 2008. **26**(8): p. 434-441.
15. Kutcher, M.E. and I.M. Herman, *The pericyte: cellular regulator of microvascular blood flow*. Microvascular research, 2009. **77**(3): p. 235-246.
16. Freedman, S.B. and J.M. Isner, *Therapeutic angiogenesis for ischemic cardiovascular disease*. Journal of molecular and cellular cardiology, 2001. **33**(3): p. 379-393.
17. Nomi, M., et al., *Role of growth factors and endothelial cells in therapeutic angiogenesis and tissue engineering*. Current stem cell research & therapy, 2006. **1**(3): p. 333-343.
18. Lamalice, L., F. Le Boeuf, and J. Huot, *Endothelial cell migration during angiogenesis*. Circulation research, 2007. **100**(6): p. 782-794.
19. Hoeben, A., et al., *Vascular endothelial growth factor and angiogenesis*. Pharmacological reviews, 2004. **56**(4): p. 549-580.
20. Sun, L., Y. Bai, and G. Du, *Endothelial dysfunction—An obstacle of therapeutic angiogenesis*. Ageing research reviews, 2009. **8**(4): p. 306-313.

21. Garbern, J.C., et al., *Delivery of basic fibroblast growth factor with a pH-responsive, injectable hydrogel to improve angiogenesis in infarcted myocardium*. *Biomaterials*, 2011. **32**(9): p. 2407-2416.
22. Censi, R., et al., *Hydrogels for protein delivery in tissue engineering*. *Journal of Controlled Release*, 2012. **161**(2): p. 680-692.
23. Chung, Y.-I., et al., *Efficient revascularization by VEGF administration via heparin-functionalized nanoparticle–fibrin complex*. *Journal of Controlled Release*, 2010. **143**(3): p. 282-289.
24. Huang, M., et al., *Polyelectrolyte complexes stabilize and controllably release vascular endothelial growth factor*. *Biomacromolecules*, 2007. **8**(5): p. 1607-1614.
25. des Rieux, A., et al., *3D systems delivering VEGF to promote angiogenesis for tissue engineering*. *Journal of Controlled Release*, 2011. **150**(3): p. 272-278.
26. Albani, D., et al., *Hydrogel-Based Nanocomposites and Mesenchymal Stem Cells: A Promising Synergistic Strategy for Neurodegenerative Disorders Therapy*. *The Scientific World Journal*, 2013. **2013**.
27. Nguyen, M.K. and D.S. Lee, *Injectable biodegradable hydrogels*. *Macromolecular bioscience*, 2010. **10**(6): p. 563-579.
28. Tan, H. and K.G. Marra, *Injectable, biodegradable hydrogels for tissue engineering applications*. *Materials*, 2010. **3**(3): p. 1746-1767.
29. Plotkin, M., et al., *The effect of matrix stiffness of injectable hydrogels on the preservation of cardiac function after a heart attack*. *Biomaterials*, 2014. **35**(5): p. 1429-1438.
30. Chung, H.J. and T.G. Park, *Self-assembled and nanostructured hydrogels for drug delivery and tissue engineering*. *Nano Today*, 2009. **4**(5): p. 429-437.

31. Bhang, S.H., et al., *Angiogenesis in ischemic tissue produced by spheroid grafting of human adipose-derived stromal cells*. *Biomaterials*, 2011. **32**(11): p. 2734-2747.
32. Russo, V., et al., *Mesenchymal stem cell delivery strategies to promote cardiac regeneration following ischemic injury*. *Biomaterials*, 2014. **35**(13): p. 3956-3974.
33. Hoffman, A.S., *Hydrogels for biomedical applications*. *Advanced drug delivery reviews*, 2012. **64**: p. 18-23.
34. Macaya, D. and M. Spector, *Injectable hydrogel materials for spinal cord regeneration: a review*. *Biomedical materials*, 2012. **7**(1): p. 012001.
35. Wan, J., *Microfluidic-based synthesis of hydrogel particles for cell microencapsulation and cell-based drug delivery*. *Polymers*, 2012. **4**(2): p. 1084-1108.
36. Lin, C.-C. and K.S. Anseth, *PEG hydrogels for the controlled release of biomolecules in regenerative medicine*. *Pharmaceutical research*, 2009. **26**(3): p. 631-643.
37. Ye, Z., et al., *Myocardial regeneration: Roles of stem cells and hydrogels*. *Advanced drug delivery reviews*, 2011. **63**(8): p. 688-697.
38. Lee, K.Y. and D.J. Mooney, *Alginate: properties and biomedical applications*. *Progress in polymer science*, 2012. **37**(1): p. 106-126.
39. Lee, J. and K.Y. Lee, *Local and sustained vascular endothelial growth factor delivery for angiogenesis using an injectable system*. *Pharmaceutical research*, 2009. **26**(7): p. 1739-1744.

40. Hao, X., et al., *Angiogenic effects of sequential release of VEGF-A165 and PDGF-BB with alginate hydrogels after myocardial infarction*. Cardiovascular Research, 2007. **75**(1): p. 178-185.
41. Silva, E. and D. Mooney, *Spatiotemporal control of vascular endothelial growth factor delivery from injectable hydrogels enhances angiogenesis*. Journal of Thrombosis and Haemostasis, 2007. **5**(3): p. 590-598.
42. Peters MC, I.B., Rowley JA, Mooney DJ., *Release from alginate enhances the biological activity of vascular endothelial growth factor*. Journal of Biomaterials Science, Polymer Edition, 1998. **9**(12): p. 1267-78.
43. Hersel, U., C. Dahmen, and H. Kessler, *RGD modified polymers: biomaterials for stimulated cell adhesion and beyond*. Biomaterials, 2003. **24**(24): p. 4385-4415.
44. Yu, J., et al., *The effect of injected RGD modified alginate on angiogenesis and left ventricular function in a chronic rat infarct model*. Biomaterials, 2009. **30**(5): p. 751-756.
45. Ricard-Blum, S., *The collagen family*. Cold Spring Harbor perspectives in biology, 2011. **3**(1): p. a004978.
46. Lee, K.Y. and D.J. Mooney, *Hydrogels for tissue engineering*. Chemical reviews, 2001. **101**(7): p. 1869-1880.
47. Drury, J.L. and D.J. Mooney, *Hydrogels for tissue engineering: scaffold design variables and applications*. Biomaterials, 2003. **24**(24): p. 4337-4351.
48. Miyagi, Y., et al., *Biodegradable collagen patch with covalently immobilized VEGF for myocardial repair*. Biomaterials, 2011. **32**(5): p. 1280-1290.
49. Elzoghby, A.O., *Gelatin-based nanoparticles as drug and gene delivery systems: reviewing three decades of research*. Journal of Controlled Release, 2013. **172**(3): p. 1075-1091.

50. Young, S., et al., *Gelatin as a delivery vehicle for the controlled release of bioactive molecules*. Journal of Controlled Release, 2005. **109**(1): p. 256-274.
51. Thompson, J., et al., *Site-directed neovessel formation in vivo*. Science, 1988. **241**(4871): p. 1349-1352.
52. Tabata, Y., et al., *Controlled release of vascular endothelial growth factor by use of collagen hydrogels*. Journal of Biomaterials Science, Polymer Edition, 2000. **11**(9): p. 915-930.
53. Tabata, Y., A. Nagano, and Y. Ikada, *Biodegradation of hydrogel carrier incorporating fibroblast growth factor*. Tissue engineering, 1999. **5**(2): p. 127-138.
54. Patel, Z.S., et al., *In vitro and in vivo release of vascular endothelial growth factor from gelatin microparticles and biodegradable composite scaffolds*. Pharmaceutical research, 2008. **25**(10): p. 2370-2378.
55. Tabata, Y. and Y. Ikada, *Vascularization effect of basic fibroblast growth factor released from gelatin hydrogels with different biodegradabilities*. Biomaterials, 1999. **20**(22): p. 2169-2175.
56. Matsui, M. and Y. Tabata, *Enhanced angiogenesis by multiple release of platelet-rich plasma contents and basic fibroblast growth factor from gelatin hydrogels*. Acta biomaterialia, 2012. **8**(5): p. 1792-1801.
57. Marui, A., et al., *A novel approach to therapeutic angiogenesis for patients with critical limb ischemia by sustained release of basic fibroblast growth factor using biodegradable gelatin hydrogel: an initial report of the phase I-IIa study*. Circulation journal: official journal of the Japanese Circulation Society, 2007. **71**(8): p. 1181-1186.

58. Pieper, J., et al., *Loading of collagen-heparan sulfate matrices with bFGF promotes angiogenesis and tissue generation in rats*. Journal of biomedical materials research, 2002. **62**(2): p. 185-194.
59. West, D.C. and S. Kumar, *The effect of hyaluronate and its oligosaccharides on endothelial cell proliferation and monolayer integrity*. Experimental cell research, 1989. **183**(1): p. 179-196.
60. Xin, X., et al., *Hyaluronic-acid-based semi-interpenetrating materials*. Journal of Biomaterials Science, Polymer Edition, 2004. **15**(9): p. 1223-1236.
61. Burdick, J.A. and G.D. Prestwich, *Hyaluronic acid hydrogels for biomedical applications*. Advanced materials, 2011. **23**(12): p. H41-H56.
62. Abdalla, S., et al., *Hyaluronic acid-based hydrogel induces neovascularization and improves cardiac function in a rat model of myocardial infarction*. Interactive cardiovascular and thoracic surgery, 2013. **17**(5): p. 767-772.
63. Linnes, M.P., B.D. Ratner, and C.M. Giachelli, *A fibrinogen-based precision microporous scaffold for tissue engineering*. Biomaterials, 2007. **28**(35): p. 5298-5306.
64. Fan, C.L., et al., *Therapeutic angiogenesis by intramuscular injection of fibrin particles into ischaemic hindlimbs*. Clinical and experimental pharmacology and physiology, 2006. **33**(7): p. 617-622.
65. Chekanov, V.S., et al., *Direct fibrin injection to promote new collateral growth in hind limb ischemia in a rabbit model*. Journal of cardiac surgery, 2002. **17**(6): p. 502-511.
66. Barreto-Ortiz, S.F., Q. Smith, and S. Gerecht, *Vascular Development and Morphogenesis in Biomaterials*. Vascularization: Regenerative Medicine and Tissue Engineering, 2014: p. 85.

67. Laschke, M., et al., *Incorporation of growth factor containing Matrigel promotes vascularization of porous PLGA scaffolds*. Journal of Biomedical Materials Research Part A, 2008. **85**(2): p. 397-407.
68. Schumann, P., et al., *Accelerating the early angiogenesis of tissue engineering constructs in vivo by the use of stem cells cultured in matrigel*. Journal of Biomedical Materials Research Part A, 2014. **102**(6): p. 1652-1662.
69. Tian, L. and S.C. George, *Biomaterials to prevascularize engineered tissues*. Journal of cardiovascular translational research, 2011. **4**(5): p. 685-698.
70. Dash, M., et al., *Chitosan—A versatile semi-synthetic polymer in biomedical applications*. Progress in polymer science, 2011. **36**(8): p. 981-1014.
71. Liu, Z., et al., *The influence of chitosan hydrogel on stem cell engraftment, survival and homing in the ischemic myocardial microenvironment*. Biomaterials, 2012. **33**(11): p. 3093-3106.
72. Wang, H., et al., *Injectable cardiac tissue engineering for the treatment of myocardial infarction*. Journal of cellular and molecular medicine, 2010. **14**(5): p. 1044-1055.
73. Zhang, S., et al., *Self-complementary oligopeptide matrices support mammalian cell attachment*. Biomaterials, 1995. **16**(18): p. 1385-1393.
74. Sieminski, A., et al., *Primary sequence of ionic self-assembling peptide gels affects endothelial cell adhesion and capillary morphogenesis*. Journal of Biomedical Materials Research Part A, 2008. **87**(2): p. 494-504.
75. Leon, E.J., et al., *Mechanical properties of a self-assembling oligopeptide matrix*. Journal of Biomaterials Science, Polymer Edition, 1998. **9**(3): p. 297-312.

76. Caplan, M.R., et al., *Control of self-assembling oligopeptide matrix formation through systematic variation of amino acid sequence*. *Biomaterials*, 2002. **23**(1): p. 219-227.
77. Narmoneva, D.A., et al., *Self-assembling short oligopeptides and the promotion of angiogenesis*. *Biomaterials*, 2005. **26**(23): p. 4837-4846.
78. Kim, J.H., et al., *The enhancement of mature vessel formation and cardiac function in infarcted hearts using dual growth factor delivery with self-assembling peptides*. *Biomaterials*, 2011. **32**(26): p. 6080-6088.
79. García, A.J., *PEG–Maleimide Hydrogels for Protein and Cell Delivery in Regenerative Medicine*. *Annals of biomedical engineering*, 2014. **42**(2): p. 312-322.
80. Liu, S.Q., et al., *Biodegradable poly (ethylene glycol)–peptide hydrogels with well-defined structure and properties for cell delivery*. *Biomaterials*, 2009. **30**(8): p. 1453-1461.
81. Kraehenbuehl, T.P., et al., *Cell-responsive hydrogel for encapsulation of vascular cells*. *Biomaterials*, 2009. **30**(26): p. 4318-4324.
82. Kavanagh, C., et al., *Poly (N-isopropylacrylamide) copolymer films as vehicles for the sustained delivery of proteins to vascular endothelial cells*. *Journal of Biomedical Materials Research Part A*, 2005. **72**(1): p. 25-35.
83. Li, F., et al., *Cellular and nerve regeneration within a biosynthetic extracellular matrix for corneal transplantation*. *Proceedings of the National Academy of Sciences*, 2003. **100**(26): p. 15346-15351.
84. Ohya, S., Y. Nakayama, and T. Matsuda, *Thermoresponsive artificial extracellular matrix for tissue engineering: hyaluronic acid bioconjugated with poly (N-isopropylacrylamide) grafts*. *Biomacromolecules*, 2001. **2**(3): p. 856-863.

85. Ohya, S. and T. Matsuda, *Poly (N-isopropylacrylamide)(PNIPAM)-grafted gelatin as thermoresponsive three-dimensional artificial extracellular matrix: molecular and formulation parameters vs. cell proliferation potential*. Journal of Biomaterials Science, Polymer Edition, 2005. **16**(7): p. 809-827.
86. Kim, S., et al., *Synthetic MMP-13 degradable ECMs based on poly (N-isopropylacrylamide-co-acrylic acid) semi-interpenetrating polymer networks. I. Degradation and cell migration*. Journal of Biomedical Materials Research Part A, 2005. **75**(1): p. 73-88.
87. Simón-Yarza, T., et al., *Vascular endothelial growth factor-delivery systems for cardiac repair: an overview*. 2012.
88. Vilos, C. and L. Velasquez, *Therapeutic strategies based on polymeric microparticles*. BioMed Research International, 2012. **2012**.
89. Golub, J.S., et al., *Sustained VEGF delivery via PLGA nanoparticles promotes vascular growth*. American Journal of Physiology-Heart and Circulatory Physiology, 2010. **298**(6): p. H1959-H1965.
90. Lee, J., et al., *Active blood vessel formation in the ischemic hindlimb mouse model using a microsphere/hydrogel combination system*. Pharmaceutical research, 2010. **27**(5): p. 767-774.
91. Coester, C., et al., *Gelatin nanoparticles by two step desolvation a new preparation method, surface modifications and cell uptake*. Journal of microencapsulation, 2000. **17**(2): p. 187-193.
92. Balthasar, S., et al., *Preparation and characterisation of antibody modified gelatin nanoparticles as drug carrier system for uptake in lymphocytes*. Biomaterials, 2005. **26**(15): p. 2723-2732.

93. Kumari, A., S.K. Yadav, and S.C. Yadav, *Biodegradable polymeric nanoparticles based drug delivery systems*. Colloids and Surfaces B: Biointerfaces, 2010. **75**(1): p. 1-18.
94. Azimi, B., et al., *Producing gelatin nanoparticles as delivery system for bovine serum albumin*. Iranian biomedical journal, 2014. **18**(1): p. 34.
95. Won, Y.-W. and Y.-H. Kim, *Recombinant human gelatin nanoparticles as a protein drug carrier*. Journal of Controlled Release, 2008. **127**(2): p. 154-161.
96. Li, J.K., N. Wang, and X.S. Wu, *A novel biodegradable system based on gelatin nanoparticles and poly (lactic-co-glycolic acid) microspheres for protein and peptide drug delivery*. Journal of pharmaceutical sciences, 1997. **86**(8): p. 891-895.
97. Wang, H., et al., *Combined delivery of BMP-2 and bFGF from nanostructured colloidal gelatin gels and its effect on bone regeneration in vivo*. Journal of Controlled Release, 2013. **166**(2): p. 172-181.
98. Walter, M.V. and M. Malkoch, *Simplifying the synthesis of dendrimers: accelerated approaches*. Chemical Society Reviews, 2012. **41**(13): p. 4593-4609.
99. Svenson, S., *Dendrimers as versatile platform in drug delivery applications*. European Journal of Pharmaceutics and Biopharmaceutics, 2009. **71**(3): p. 445-462.
100. Liu, M. and J.M. Fréchet, *Designing dendrimers for drug delivery*. Pharmaceutical science & technology today, 1999. **2**(10): p. 393-401.
101. Camci-Unal, G., et al., *Synthesis and characterization of hybrid hyaluronic acid-gelatin hydrogels*. Biomacromolecules, 2013. **14**(4): p. 1085-1092.

102. Meyvis, T.K., et al., *A comparison between the use of dynamic mechanical analysis and oscillatory shear rheometry for the characterisation of hydrogels*. International journal of pharmaceutics, 2002. **244**(1): p. 163-168.
103. Gloria, A., et al., *Rheological characterization of hyaluronic acid derivatives as injectable materials toward nucleus pulposus regeneration*. Journal of biomaterials applications, 2012. **26**(6): p. 745-759.
104. Giordano, C., et al., *Nanocomposites for neurodegenerative diseases: hydrogel-nanoparticle combinations for a challenging drug delivery*. The International journal of artificial organs, 2011. **34**(12): p. 1115-1127.
105. Russo, T., et al., *Poly (ϵ -caprolactone) reinforced with sol-gel synthesized organic-inorganic hybrid fillers as composite substrates for tissue engineering*. Journal of Applied Biomaterial and Biomechanics, 2010. **8**(3): p. 146.
106. Domingos, M., et al., *The first systematic analysis of 3D rapid prototyped poly (ϵ -caprolactone) scaffolds manufactured through BioCell printing: the effect of pore size and geometry on compressive mechanical behaviour and in vitro hMSC viability*. Biofabrication, 2013. **5**(4): p. 045004.
107. Bussolino, F., et al., *Granulocyte-and granulocyte-macrophage-colony stimulating factors induce human endothelial cells to migrate and proliferate*. Nature, 1989. **337**(6206): p. 471-473.
108. Russo, T., et al., *Hydrogels for central nervous system therapeutic strategies*. Proceedings of the Institution of Mechanical Engineers, Part H: Journal of Engineering in Medicine, 2015. **229**(12): p. 905-916.